

THESIS FOR THE DEGREE OF LICENTIATE OF ENGINEERING

# On Adaptive Finite Element Methods Based on A Posteriori Error Estimates

Axel Målqvist

**CHALMERS** | GÖTEBORG UNIVERSITY



Department of Computational Mathematics  
Chalmers University of Technology and Göteborg University  
Göteborg, Sweden 2004

On Adaptive Finite Element Methods Based on A Posteriori Error Estimates

Axel Målqvist

©Axel Målqvist, 2004

NO 2004-15

ISSN 0347-2809

Department of Computational Mathematics  
Chalmers University of Technology and Göteborg University  
SE-412 96 Göteborg  
Sweden  
Telephone +46 (0)31 772 1000

Printed in Göteborg, Sweden 2004

# On Adaptive Finite Element Methods Based on A Posteriori Error Estimates

**Axel Målqvist**

Department of Computational Mathematics  
Chalmers University of Technology  
Göteborg University

## **Abstract**

In this thesis we develop a posteriori error estimation techniques and adaptive algorithms for finite element approximations of second order problems in three different applications. The adaptive algorithms are used for automatic tuning of critical parameters in the finite element method.

First we consider the boundary penalty method for weakly imposing Dirichlet boundary conditions. We prove error estimates in the  $L^2$  and energy norms and use these to relate the penalty parameter to the mesh parameter.

Second we study the Galerkin least-squares method for minimizing pollution when solving the Helmholtz equation. We show how existing methods derived for structured grids needs to be modified to work on unstructured grids. Again the analysis is based on a posteriori error estimates.

Finally, we develop a framework for a posteriori error estimation in multiscale problems. We present a method for solving decoupled localized fine scale problems on patches and an a posteriori error estimate that relates the coarse scale mesh size, the fine scale mesh size, and the patch size.

**Keywords:** finite element method, Galerkin, duality, a posteriori error estimation, adaptivity, Poisson equation, boundary penalty method, Helmholtz equation, pollution, variational multiscale method



## Acknowledgements

First of all I would like to thank my advisor Assoc. Prof. Mats G. Larson for interesting topics, inspirational talks, and for the constant stream of good ideas he has put into my projects. I am thankful to have met Mats at a very crucial point in my career.

I also would like to thank my co-advisor Prof. Kenneth Eriksson who lead me into the path of finite elements and error estimation many years ago when I still was an undergraduate student at Chalmers.

I am also thankful and indebted to Prof. Claes Johnson for giving me the opportunity to work as a PhD student in his group.

I would like to thank all my colleagues at the finite element center for providing such a nice working environment, in particular the talented Anders Logg, who has also helped me with computer issues, and my former roommate Georgios Foufas who has become a true friend to me.

Outside this group two friends have been a constant inspiration and motivation for me to get the most out of my work and life, thanks Per Sundell and Erik Broman.

Finally, I would like thank my family in Aneby and Stockholm for making my life so easy to live. I am a happy guy who has his rough days rather than vice versa thanks to you.



**This thesis consists of the following papers:**

**Paper I:** *A Posteriori Error Analysis of the Boundary Penalty Method*, Finite Element Center Preprint 2004-09. (Submitted)

The Boundary Penalty Method enforces Dirichlet boundary conditions weakly by a penalty parameter. We derive a posteriori error estimates in the  $L^2(\Omega)$ -norm and energy semi-norm for this method and we propose an adaptive strategy to choose the penalty parameter  $\epsilon$  and the mesh parameter  $h$  by equidistributing the error between the terms in the energy semi-norm estimate. Finally, we consider three numerical examples where we successfully use the adaptive algorithm to solve the Poisson equation with both smooth and non-smooth boundary data.

**Paper II:** *A Posteriori Error Analysis of Stabilized Finite Element Approximations of the Helmholtz Equation on Unstructured Grids*, Finite Element Center Preprint 2004-10. (Submitted)

In this paper we study the Galerkin least-squares method for minimizing pollution when solving Helmholtz equation. We especially consider how stochastic perturbations on a structured mesh affects the optimal choice of the method parameter  $\tau$ . The analysis is based on an error representation formula derived by a posteriori error estimates using duality. The primary goal with this work is not to present a brand new method for this problem but to show how existing methods derived for structured meshes can be modified to work on unstructured grids. We conclude that a parameter optimized for a structured mesh needs to be increased by a term proportional to the variance of the perturbation to be unbiased on a perturbed grid. We present numerical examples in one and two dimensions to confirm our theoretical results.

**Paper III:** *Adaptive Variational Multiscale Method Based on A Posteriori Error Estimates*, Finite Element Center Preprint 2004-11. (Submitted)

The variational multiscale method (VMM) provides a general framework for construction of multiscale finite element methods. In this paper we propose a method for parallel solution of the fine scale problem based on localized Dirichlet problems which are solved numerically. Next we present a posteriori error estimates for VMM which relates the error in linear functionals and the energy norm to the discretization errors, resolution and size of patches in the localized problems, in the fine scale approximation. Based on the a posteriori error estimates we propose an adaptive VMM with automatic tuning of the critical parameters. We study elliptic second order partial differential equations with highly oscillating coefficients or localized singularities.



# A Posteriori Error Analysis of the Boundary Penalty Method

Kenneth Eriksson\*, Mats G. Larson† and Axel Målqvist‡

April 7, 2004

## Abstract

The Boundary Penalty Method enforces Dirichlet boundary conditions weakly by a penalty parameter. We derive a posteriori error estimates in the  $L^2(\Omega)$ -norm and energy semi-norm for this method and we propose an adaptive strategy to choose the penalty parameter  $\epsilon$  and the mesh parameter  $h$  by equidistributing the error between the terms in the energy semi-norm estimate. Finally, we consider three numerical examples where we successfully use the adaptive algorithm to solve the Poisson equation with both smooth and non-smooth boundary data.

## 1 Introduction

**The Boundary Penalty Method.** The Boundary Penalty Method (BPM) has been known and used for more than thirty years. The basic idea is to impose Dirichlet boundary conditions weakly by using Robin type boundary condition with a penalty parameter  $\epsilon$ . We consider the following model problem: find  $u$  such that

$$\begin{cases} -\Delta u = f & \text{in } \Omega, \\ u = g & \text{on } \Gamma, \end{cases} \quad (1.1)$$

where  $\Omega$  is a polygonal domain in  $\mathbf{R}^d$ ,  $d = 1, 2$  or  $3$ , with boundary  $\Gamma$ . Further  $f \in H^{-1}(\Omega)$  and  $g \in H^{1/2}(\Gamma)$  are given data, see [1] for definitions

---

\*Professor, Department of Informatics and Mathematics, University of Trollhättan Uddevalla, Trollhättan, kenneth.eriksson@htu.se.

†Corresponding author, Associate Professor, Department of Mathematics, Chalmers University of Technology, Göteborg, mgl@math.chalmers.se.

‡Graduate Research Assistant, Department of Mathematics, Chalmers University of Technology, Göteborg, axel@math.chalmers.se.

of these spaces. The finite element formulation using BPM [3, 4] now reads: find  $U \in V$  such that

$$(\nabla U, \nabla v) + (\epsilon^{-1}U, v)_\Gamma = (f, v) + (\epsilon^{-1}g, v)_\Gamma \quad \text{for all } v \in V, \quad (1.2)$$

where  $(\cdot, \cdot)$  is the  $L^2(\Omega)$  scalar product,  $(\cdot, \cdot)_\Gamma$  is the  $L^2(\Gamma)$  scalar product, and  $V \subset H^1(\Omega)$  is the space of continuous piecewise polynomials of degree  $p$  with respect to a given triangulation  $\mathcal{K} = \{K\}$  of  $\Omega$  into elements  $K$  of diameter  $h_K$ . We define the mesh function (mesh parameter)  $h(x)$  such that  $h(x) = h_K$  when  $x \in K$ . We assume that the mesh is locally quasi-uniform.

We immediately note that this method is not consistent since  $u$  does not solve equation (1.2). Multiplying equation (1.1) with a test function and integrating over the domain using Green's formula gives the following identity for the exact solution  $u$ ,

$$(\nabla u, \nabla v) - (\partial_n u, v)_\Gamma = (f, v) \quad \text{for all } v \in H^1(\Omega), \quad (1.3)$$

where  $\partial_n u = n \cdot \nabla u$  is the normal derivative of  $u$ . However, there is a more complicated method for weakly imposing Dirichlet boundary conditions called Nitsche's method [15, 12] which is consistent. The idea in this method is to include the term  $(\partial_n U, v)_\Gamma$  that appears in equation (1.3) in equation (1.2) together with a compensating term that makes the method symmetric.

Both BPM and Nitsche's method have been used for problems with interior sub-domain interfaces. One of the first papers on the interior penalty method is Babuška [2] from 1970. In a recent paper [14] this method has been used for gluing together non-matching grids.

There are various reasons for studying the BPM. One is that it allows Dirichlet ( $\epsilon$  small), Neumann ( $\epsilon$  large), and Robin ( $\epsilon$  as a function on  $\Gamma$ ) boundary conditions in the same framework. It is also very easy to implement and it has for these reasons been used in many finite element codes over the years. Another reason for studying this method is that it serves as a simpler compliment to Nitsche's method e.g. when solving problems on non-matching grids. As mentioned before Lazarov et.al. [14] chooses this method in their work on non-matching grids.

**Previous Work.** One of the first works on this subject is Babuška [3] from 1973. His results was then improved and extended among others by Barrett and Elliott [4] during the eighties. Their work are all in an a priori setting and has inspired us to do an a posteriori error analysis of this method. Some important results from these papers are that for piecewise linears  $\epsilon = h$  in the boundary penalty formulation, equation (1.2), yields an optimal  $H^1(\Omega)$  error estimate but this choice leads to a suboptimal  $L^2(\Omega)$  error estimate.

As mentioned earlier BPM is not a consistent method i.e. (1.2) will not hold if  $U$  is replaced by  $u$ . For higher order polynomials this will force the penalty parameter  $\epsilon$  be proportional to a higher power of  $h$ . The reason why  $\epsilon \sim h$  is desired is that this choice will not affect the condition number of the stiffness matrix. High condition number leads to slow convergence for iterative solvers. For higher order base functions Nitsche's method is optimal for  $\epsilon \sim h$ .

As far as we know this is the first a posteriori paper on the boundary penalty method. However, there are several related papers on a posteriori error estimates for discontinuous Galerkin and non-conforming finite element methods [8, 5, 12].

**New Contributions.** The aim of this paper is to derive an a posteriori error estimate in terms of the mesh parameter  $h$  and the penalty parameter  $\epsilon$ , and based on these results construct an adaptive algorithm to solve problem (1.2) efficiently.

Our main results are the following bounds of the energy and  $L^2(\Omega)$  norm of the error  $e = u - U$ :

$$\|\nabla e\| \leq C (\|hR(U)\| + \|g - U\|_{1/2,\Gamma}), \quad (1.4)$$

$$\|e\| \leq C (\|h^2R(U)\| + \|g - U\|_{-1/2,\Gamma}), \quad (1.5)$$

where  $\|\cdot\|_{s,\Gamma}$  is the  $H^s(\Gamma)$  norm,  $R(U)$  is a computable bound of the residual,  $f + \Delta U \in H^{-1}(\Omega)$ , on  $\Omega$ , and  $C$  denotes throughout this paper various constants independent of  $h$  and  $\epsilon$ .

To design an adaptive algorithm from the energy semi-norm estimates we need to see explicitly how the a posteriori quantity  $\|g - U\|_{1/2,\Gamma}$  depends on  $\epsilon$ . We introduce  $P$  as the  $L^2(\Gamma)$  projection onto the restriction of  $V$  on  $\Gamma$  and get,

$$\|Pg - U\|_{1/2,\Gamma} \leq C\epsilon \left( \|P(\partial_n U)\|_{1/2,\Gamma} + \sum_{\partial K \cap \Gamma \neq \emptyset} \|R(U)\|_K \right). \quad (1.6)$$

Combining equation (1.4) and equation (1.6) yields the final error estimate that will be used for the adaptive algorithm,

$$\begin{aligned} \|\nabla e\| &\leq C (\|hR(U)\| + \|g - Pg\|_{1/2,\Gamma}) \\ &+ C\epsilon \left( \|P(\partial_n U)\|_{1/2,\Gamma} + \sum_{\partial K \cap \Gamma \neq \emptyset} \|R(U)\|_K \right). \end{aligned} \quad (1.7)$$

Obviously there exists an upper bound on  $\epsilon$  in equation (1.2) for which the approximation gets to poor. We can capture this bound by considering

the error estimate in equation (1.7). We also need to impose a lower bound on  $\epsilon$  for at least two reasons: the condition number of the stiffness matrix grows when  $\epsilon$  decreases, and we may get undesired oscillations in the solution when solving problems with rough boundary data (see Example 3 in section 4). The conclusion of this discussion is that  $\epsilon$  needs to be small enough to balance the two terms in equation (1.7) but not smaller.

We also present an estimate of the term  $\|Pg - U\|_{-1/2,\Gamma}$  in the  $L^2(\Omega)$ -norm bound, see equation (1.5), and by using this estimate we get the following bound of the  $L^2(\Omega)$ -norm of the error,

$$\|e\| \leq C (\|(h^2 + \epsilon h + \epsilon^2)R(U)\| + \|g - Pg\|_{-1/2,\Gamma} + \epsilon\|g - Pg\|_{1/2,\Gamma}) \quad (1.8) \\ + \epsilon C (\|P(\partial_n U)\|_{-1/2,\Gamma} + \epsilon\|P(\partial_n U)\|_{1/2,\Gamma}).$$

Here we see that  $\epsilon \sim h$  is not enough to get an optimal order error estimate since the estimate contains the term  $\epsilon\|P(\partial_n U)\|_{-1/2,\Gamma}$ .

In this work we consider piecewise linear approximations since in this case have an optimal a priori estimate in the energy semi-norm. We are not interested in tracking the constants in the error estimates.

**Outline.** In Section 2, we present the a posteriori error analysis for control in energy semi-norm and  $L^2(\Omega)$ -norm. In Section 3 we use the error estimates to derive an adaptive algorithm for choosing the penalty parameter. In Section 4 we present three numerical examples, and finally we present a small summary in Section 5.

## 2 A Posteriori Error Estimates

### 2.1 The Error Representation Formula

Subtracting (1.2) from (1.3) yields the error equation

$$(\nabla e, \nabla v) + (\epsilon^{-1}e, v)_\Gamma = (\partial_n u, v)_\Gamma \quad \text{for all } v \in V. \quad (2.1)$$

Green's formula gives,

$$(f + \Delta U, v) + (\partial_n e + \epsilon^{-1}e, v)_\Gamma = (\partial_n u, v)_\Gamma \quad \text{for all } v \in V, \quad (2.2)$$

where the first scalar product is defined in the following way,

$$(f + \Delta U, v) = \sum_K \int_K (f + \Delta U)v \, dx - \sum_K \int_{\partial K \setminus \Gamma} \frac{\partial U}{\partial n_K} v \, ds. \quad (2.3)$$

We also need to take weighted  $L^2(\Omega)$  norms of  $f + \Delta U$ . We define our domain residual according to [10] as a piecewise constant function,

$$R(U) = |f + \Delta U| + \frac{1}{2} \max_{\partial K \setminus \Gamma} h_K^{-1} |[\partial_n U]| \quad \text{on } K \in \mathcal{K}, \quad (2.4)$$

where  $[\cdot]$  is the difference in the function value over the edge. We note that  $|(f + \Delta U, v)| \leq \|h^s R(U)\| \|h^{-s} v\|$  for  $s \in \mathbf{R}$ . Next we introduce a dual problem: find  $\phi$  such that

$$\begin{cases} -\Delta \phi = \psi & \text{in } \Omega, \\ \phi = 0 & \text{on } \Gamma, \end{cases} \quad (2.5)$$

where  $\psi \in H^{-1}(\Omega)$ . Multiplying (2.5) by the error  $e$  and using Green's formula yields,

$$(e, \psi) = (e, -\Delta \phi) = (\nabla e, \nabla \phi) - (e, \partial_n \phi)_\Gamma = (f + \Delta U, \phi) - (g - U, \partial_n \phi)_\Gamma. \quad (2.6)$$

It follows from equation (2.2) that  $(f + \Delta U, v) = 0$  for  $v \in V$  such that  $v = 0$  on  $\Gamma$ . We then get  $(f + \Delta U, \pi \phi) = 0$ , where  $\pi \phi$  is the Scott-Zhang interpolant of  $\phi$ , see [6]. Together this gives,

$$\boxed{(e, \psi) = (f + \Delta U, \phi - \pi \phi) - (g - U, \partial_n \phi)_\Gamma} \quad (2.7)$$

## 2.2 The Error Estimates

We start this section by proving estimates of the error in energy and  $L^2(\Omega)$  norm.

**Theorem 2.1** *It holds*

$$\boxed{\|\nabla e\| \leq C (\|hR(U)\| + \|g - U\|_{1/2, \Gamma})} \quad (2.8)$$

*If we assume that there exists a constant  $C$  such that  $\|\phi\|_2 \leq C\|\Delta \phi\|$  we also have*

$$\boxed{\|e\| \leq C (\|h^2 R(U)\| + \|g - U\|_{-1/2, \Gamma})} \quad (2.9)$$

**Proof.** For the energy semi-norm estimate we start from equation (2.7) and let  $\psi = -\Delta e$ ,

$$(e, -\Delta e) = (f + \Delta U, \phi - \pi \phi) - (g - U, \partial_n \phi)_\Gamma. \quad (2.10)$$

We have  $(e, -\Delta e) = \|\nabla e\|^2 - (e, \partial_n e)_\Gamma$  and together with equation (2.10) this gives

$$\|\nabla e\|^2 = (f + \Delta U, \phi - \pi\phi) - (e, \partial_n \phi)_\Gamma + (e, \partial_n e)_\Gamma \quad (2.11)$$

$$\leq C (\|hR(U)\| \|\nabla \phi\| + \|e\|_{1/2, \Gamma} \|\partial_n \phi\|_{-1/2, \Gamma} + \|e\|_{1/2, \Gamma} \|\partial_n e\|_{-1/2, \Gamma}). \quad (2.12)$$

We recall the trace inequality,

$$\|n \cdot v\|_{-1/2, \Gamma} \leq C \sum_{\partial K \cap \Gamma \neq \emptyset} (\|v\|_K + h \|\nabla \cdot v\|_K), \quad (2.13)$$

where  $\|\cdot\|_K$  is the  $L^2(K)$  norm where  $K$  refers to elements in the mesh, see ([11], Theorem 2.2) and apply this result twice with  $v = \nabla \phi$  and  $v = \nabla e$  on equation (2.12) to get,

$$\begin{aligned} \|\nabla e\|^2 &\leq \frac{1}{2} C^2 \|hR(U)\|^2 + \frac{1}{2} \|\nabla \phi\|^2 + \|e\|_{1/2, \Gamma} \sum_{\partial K \cap \Gamma \neq \emptyset} (\|\nabla e\|_K + \|hR(U)\|_K) \\ &\quad + \|e\|_{1/2, \Gamma} \sum_{\partial K \cap \Gamma \neq \emptyset} (\|\nabla \phi\|_K + \|hR(U)\|_K). \end{aligned} \quad (2.14)$$

Next we use the following observation,

$$\|\nabla \phi\|^2 = (-\Delta e, \phi) = (\nabla e, \nabla \phi) \leq \|\nabla e\| \|\nabla \phi\|, \quad (2.15)$$

i.e.  $\|\nabla \phi\| \leq \|\nabla e\|$  to get,

$$\|\nabla e\|^2 \leq C \|hR(U)\|^2 + \frac{1}{2} \|\nabla e\|^2 + 2 \|e\|_{1/2, \Gamma} (\|\nabla e\| + \|hR(U)\|) \quad (2.16)$$

$$\leq C \left( \|hR(U)\|^2 + \|e\|_{1/2, \Gamma}^2 \right) + \frac{3}{4} \|\nabla e\|^2. \quad (2.17)$$

Subtracting  $3/4 \|\nabla e\|^2$  on both sides proves the first part of the theorem.

For the  $L^2(\Omega)$  estimate we use  $\psi = e/\|e\|$  in (2.7) to get,

$$\|e\| = (e, \psi) = (f + \Delta U, \phi - \pi\phi) - (g - U, \partial_n \phi)_\Gamma. \quad (2.18)$$

Now we use the assumption that there exists a constant  $C$  such that  $\|\phi\|_2 \leq C \|\Delta \phi\|$  and use the trace inequality  $\|\partial_n \phi\|_{1/2} \leq C \|\phi\|_2$  to get

$$\|e\| \leq C \|h^2 R(U)\| \|\phi\|_2 + C \|g - U\|_{-1/2, \Gamma} \|\phi\|_2 \quad (2.19)$$

$$\leq C (\|h^2 R(U)\| + \|g - U\|_{-1/2, \Gamma}). \quad (2.20)$$

□

In Theorem 2.1 we get bounds with the  $\epsilon$  dependence hidden. To be able to construct an adaptive algorithm we wish to know how  $\|g - U\|_{1/2,\Gamma}$  and  $\|g - U\|_{-1/2,\Gamma}$  depends on  $\epsilon$ . We use the triangle inequality

$$\|g - U\|_{s,\Gamma} \leq \|g - Pg\|_{s,\Gamma} + \|Pg - U\|_{s,\Gamma}, \quad (2.21)$$

for  $s = 1/2$  and  $s = -1/2$ . The first part is independent of  $\epsilon$  and the second part can be estimated. We start with  $\|g - U\|_{1/2,\Gamma}$ .

**Theorem 2.2** *It holds*

$$\|Pg - U\|_{1/2,\Gamma} \leq C\epsilon \left( \|P(\partial_n U)\|_{1/2,\Gamma} + \sum_{\partial K \cap \Gamma \neq \emptyset} \|R(U)\|_K \right) \quad (2.22)$$

where  $Pg$  is the  $L^2(\Gamma)$  projection of  $g$  onto the restriction of  $V$  on the boundary.

**Proof.** We let  $z = P(\epsilon \partial_n U) \in V$  and start by using the triangle inequality,

$$\|Pg - U\|_{1/2,\Gamma} \leq \|z\|_{1/2,\Gamma} + \|Pg - U - z\|_{1/2,\Gamma} \quad (2.23)$$

$$\leq \epsilon \|P(\partial_n U)\|_{1/2,\Gamma} + C \|h^{-1/2}(Pg - U - z)\|_{\Gamma}, \quad (2.24)$$

where we use an inverse estimate [6] in the second inequality. Next we need to estimate  $\|h^{-1/2}(Pg - U - z)\|_{\Gamma}$ .

From the error equation (2.2) we have,

$$-\epsilon(f + \Delta U, v) = (g - U - \epsilon \partial_n U, v)_{\Gamma} = (Pg - U - z, v)_{\Gamma} \quad \text{for all } v \in V. \quad (2.25)$$

We let  $w \in V$  be equal to zero on interior nodes,  $w = P(h^{-1}(Pg - U - z))$  on  $\Gamma$ , and choose  $v = w$  in equation (2.25) to get,

$$\|h^{-1/2}(Pg - U - z)\|_{\Gamma}^2 = (Pg - U - z, w)_{\Gamma} \quad (2.26)$$

$$= (Pg - U - \epsilon \partial_n U, w)_{\Gamma} \quad (2.27)$$

$$= -\epsilon(f + \Delta U, w). \quad (2.28)$$

The right hand side in equation (2.26) can now be estimated in the following way,

$$|(f + \Delta U, w)| \leq C \left( \sum_{\partial K \cap \Gamma \neq \emptyset} \|R(U)\|_K \right) \|w\| \quad (2.29)$$

$$\leq C \left( \sum_{\partial K \cap \Gamma \neq \emptyset} \|R(U)\|_K \right) \|h^{-1/2}(Pg - U - z)\|_{\Gamma}. \quad (2.30)$$

We need to take a closer look at the second inequality. Let  $K$  be a triangle at the boundary and  $E$  the corresponding boundary edge of this triangle. For  $w$  as above and the finite element base functions  $\varphi_i$  we have  $\|\varphi_i^{1/2}w\|_K^2 \leq Ch_K \|\varphi_i^{1/2}w\|_E^2$ , by equivalent norms in finite dimensional spaces, and scaling. The assumption of local quasi-uniform mesh gives an estimate of  $\|w\|$  in the following way,

$$\|w\|^2 = \int_{\Omega} \left( \sum_i \varphi_i w \right)^2 \leq C \sum_i \int_{\Omega} \varphi_i^2 w^2 \leq C \sum_i \sum_{|K \cap \Gamma| \neq \emptyset} \int_K \varphi_i w^2 \quad (2.31)$$

$$\leq C \sum_i \sum_E Ch_K \|\varphi_i^{1/2}w\|_E^2 \leq \sum_E C \|h^{1/2}w\|_E^2 = C \|h^{1/2}w\|_{\Gamma}^2, \quad (2.32)$$

which means that  $\|w\| \leq C \|h^{-1/2}(Pg - U - z)\|_{\Gamma}$ . Combining equation (2.26) and equation (2.29) gives

$$\|h^{-1/2}(Pg - U - z)\|_{\Gamma} \leq C\epsilon \sum_{\partial K \cap \Gamma \neq \emptyset} \|R(U)\|_K. \quad (2.33)$$

Together equation (2.33) and equation (2.23) now gives,

$$\|Pg - U\|_{1/2, \Gamma} \leq \|z\|_{1/2, \Gamma} + C\epsilon \sum_{\partial K \cap \Gamma \neq \emptyset} \|R(U)\|_K, \quad (2.34)$$

which proves the theorem.  $\square$

Finally we close this section by finishing the  $L^2(\Omega)$ -norm estimate in the same way as we did with the energy norm estimate. From Theorem 2.1 we see that we need to estimate  $\|g - U\|_{-1/2, \Gamma}$  in terms of the mesh parameter  $h$  and  $\epsilon$ .

**Theorem 2.3** *It holds,*

$$\boxed{\|Pg - U\|_{-1/2, \Gamma} \leq \epsilon C (\|P(\partial_n U)\|_{-1/2, \Gamma} + \|\nabla e\| + \|hR(U)\|)} \quad (2.35)$$

**Proof.** We start in the same way as in the proof of Theorem 2.2. We let  $z = P(\epsilon \partial_n U) \in V$  and use the triangle inequality,

$$\|Pg - U\|_{-1/2, \Gamma} \leq \|z\|_{-1/2, \Gamma} + \|Pg - U - z\|_{-1/2, \Gamma} \quad (2.36)$$

$$\leq \epsilon \|P(\partial_n U)\|_{-1/2, \Gamma} + \|Pg - U - z\|_{-1/2, \Gamma}. \quad (2.37)$$

We study the second term equation (2.37). By definition we have,

$$\|Pg - U - z\|_{-1/2,\Gamma} = \sup_{w \in H^1(\Omega)} \frac{(Pg - U - z, w)_\Gamma}{\|w\|_{1,\Omega}} \quad (2.38)$$

$$= \sup_{w \in H^1(\Omega)} \frac{(Pg - U - z, w - Qw)_\Gamma}{\|w\|_{1,\Omega}} \quad (2.39)$$

$$+ \sup_{w \in H^1(\Omega)} \frac{(Pg - U - z, Qw)_\Gamma}{\|w\|_{1,\Omega}} \\ = I + II, \quad (2.40)$$

where  $Q$  is the  $L^2(\Omega)$ -projection onto the finite element space  $V$ . We start with the first term  $I$ ,

$$I \leq \sup_{w \in H^1(\Omega)} \frac{\|h(Pg - U - z)\|_{1/2,\Gamma} \|\frac{1}{h}(w - Qw)\|_{-1/2,\Gamma}}{\|w\|_{1,\Omega}} \quad (2.41)$$

$$\leq \|h(Pg - U - z)\|_{1/2,\Gamma} \sup_{w \in H^1(\Omega)} \frac{\|\frac{1}{h}(w - Qw)\|}{\|w\|_{1,\Omega}} \quad (2.42)$$

$$\leq C \|h(Pg - U - z)\|_{1/2,\Gamma} \quad (2.43)$$

$$\leq C \|h^{1/2}(Pg - U - z)\|_\Gamma, \quad (2.44)$$

where the last step is done by an inverse inequality [6]. By a similar argument as in the proof of Theorem 2.2, with the function  $w$  equal to  $P(h(Pg - U - z))$  on  $\Gamma$  instead we get,

$$\|h^{1/2}(Pg - U - z)\|_\Gamma \leq C \epsilon \|hR(U)\|, \quad (2.45)$$

i.e.

$$\sup_{w \in H^1(\Omega)} \frac{(Pg - U - z, w - Qw)_\Gamma}{\|w\|_{1,\Omega}} \leq C \epsilon \|hR(U)\|. \quad (2.46)$$

From equation (2.25) we have  $-\epsilon(f + \Delta U, Qw) = (Pg - U - z, Qw)_\Gamma$ . We use this result to estimate the second term  $II$  as follows,

$$II = -\epsilon \sup_{w \in H^1(\Omega)} \frac{(f + \Delta U, Qw)}{\|w\|_{1,\Omega}} \quad (2.47)$$

$$= -\epsilon \sup_{w \in H^1(\Omega)} \frac{(-\Delta e, Qw)}{\|w\|_{1,\Omega}} \quad (2.48)$$

$$= -\epsilon \sup_{w \in H^1(\Omega)} \frac{(\nabla e, \nabla Qw) - (\partial_n e, Qw)_\Gamma}{\|w\|_{1,\Omega}} \quad (2.49)$$

$$\leq \epsilon \left( \|\nabla e\| \sup_{w \in H^1(\Omega)} \frac{\|\nabla Qw\|}{\|w\|_{1,\Omega}} + \|\partial_n e\|_{-1/2,\Gamma} \sup_{w \in H^1(\Omega)} \frac{\|Qw\|_{1/2,\Gamma}}{\|w\|_{1,\Omega}} \right). \quad (2.50)$$

From [7, 9] we know that  $\|Qw\|_{1,\Omega} \leq C\|w\|_{1,\Omega}$  for locally quasi-uniform meshes. Together with the estimate,  $\|Qw\|_{1/2,\Gamma} \leq C\|Qw\|_{1,\Omega}$ , and equation (2.50) this gives,

$$\sup_{w \in H^1(\Omega)} \frac{(Pg - U - z, Qw)_\Gamma}{\|w\|_{1,\Omega}} \leq \epsilon C (\|\nabla e\| + \|\partial_n e\|_{-1/2,\Gamma}). \quad (2.51)$$

Equation (2.13) can now be used again with  $v = e$ . We get,

$$\sup_{w \in H^1(\Omega)} \frac{(Pg - U - z, Qw)_\Gamma}{\|w\|_{1,\Omega}} \leq \epsilon C (\|\nabla e\| + \|hR(U)\|). \quad (2.52)$$

Combining equation (2.37), (2.38), (2.41), and (2.52) finally proves the Theorem.  $\square$

Combining the estimate (2.9) of Theorem 2.1, Theorem 2.3, and the energy semi-norm estimate in Theorem 2.1 we finally end up with the following  $L^2(\Omega)$ -norm estimate,

$$\begin{aligned} \|e\| \leq C (\|(h^2 + \epsilon h + \epsilon^2)R(U)\| + \|g - Pg\|_{-1/2,\Gamma} + \epsilon \|g - Pg\|_{1/2,\Gamma}) \\ + \epsilon C (\|P(\partial_n U)\|_{-1/2,\Gamma} + \epsilon \|P(\partial_n U)\|_{1/2,\Gamma}). \end{aligned} \quad (2.53)$$

**Remark 2.1** In the final  $L^2(\Omega)$ -norm estimate, equation (2.53), we see that for sufficiently smooth boundary data,  $g$ , letting  $\epsilon \sim h$  would give an optimal order error for all terms but the  $\epsilon C \|P(\partial_n U)\|_{-1/2,\Gamma}$  term. So if  $\partial_n u \neq 0$  we need to let  $\epsilon \sim h^2$  to get optimal order convergence.

### 3 Adaptive Strategies

We design an adaptive strategy for the energy semi-norm estimate starting from (2.8) in Theorem 2.1. Combining this result with equation (2.21) and Theorem 2.2 gives the following equation:

$$\begin{aligned} \|\nabla e\| \leq C (\|hR(U)\| + \|g - Pg\|_{1/2,\Gamma}) \\ + C\epsilon \left( \|P(\partial_n U)\|_{1/2,\Gamma} + \sum_{\partial K \cap \Gamma \neq \emptyset} \|R(U)\|_K \right) \end{aligned} \quad (3.1)$$

We introduce the notation,

$$\begin{aligned} r_1 &= \|hR(U)\| + \|g - Pg\|_{1/2,\Gamma}, \\ r_2 &= \epsilon \left( \|P(\partial_n U)\|_{1/2,\Gamma} + \sum_{K \cap \Gamma \neq \emptyset} \|R(U)\|_K \right). \end{aligned} \quad (3.2)$$

**Adaptive Algorithm.** The aim is to choose  $\epsilon$  such that  $r_1$  and  $r_2$  becomes equally large.

- Let  $\epsilon_0 = h$ .
- Solve equation (1.2) for  $U$ .
- Calculate  $r_1$  and  $r_2$  according to equation (3.2).
- Determine if  $h$ -adaptivity is necessary from the size of  $r_1$ .
- Let  $\epsilon = \epsilon_0 \frac{r_1}{r_2}$ .

If a mesh refinement (with new mesh parameter  $h_{new}$ ) was needed in step 4 we replace  $r_1$  with  $\|h_{new}R(U)\| + \|g - Pg\|_{1/2,\Gamma}$  in step 5. This procedure can then be done iteratively going from step 5 to step 2.

**Remark 3.1** From experience and numerical tests for example in [13] we know that the first term in  $r_1$  is in general over estimated due to the inequalities used to derive it. This is not the case with the other terms and this fact could be a reason to decrease  $\epsilon$  even further. So even though in practice we want to use  $\epsilon < \epsilon_0 r_1 / r_2$  as large as possible it can be wise to choose  $\epsilon$  a bit under the bound.

**Remark 3.2** We can also use other norms for the adaptive strategy. One reason to choose the energy semi-norm is that  $\epsilon \sim h$  since  $r_1 \sim h$  and  $r_2 \sim \epsilon$ . If we instead consider the  $L^2(\Omega)$  norm we would get  $\epsilon \sim h^2$  to achieve optimal order. These results agree with earlier a priori results [6].

**Remark 3.3** The main reason for not choosing  $\epsilon$  too small is that the condition number of the stiffness matrix will be very large which leads to slow convergence for iterative solvers. The choice  $\epsilon \sim h$  is optimal since in this case the condition number of the matrix will not increase dramatically while for  $\epsilon \sim h^2$  it will. The other reason will be illustrated in Example 3 below.

## 4 Numerical Examples

We present three numerical examples to verify the theoretical results of the error analysis.

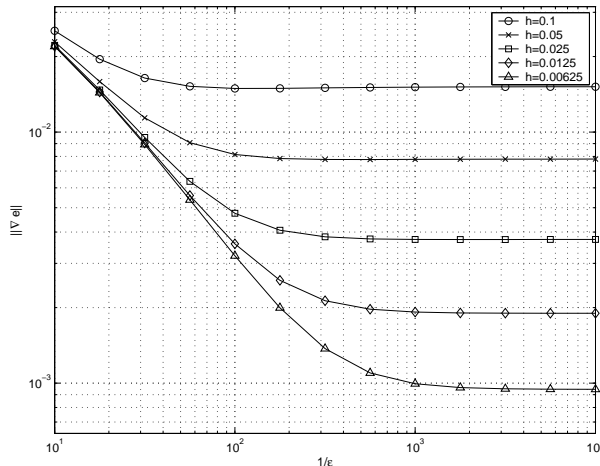


Figure 1: Error in energy semi-norm for different  $h$  and  $\epsilon$ .

**Example 1.** In the first example  $\Omega$  is the unit square and  $g = 0$  on the boundary. The load  $f$  is chosen such that the exact solution  $u(x, y) = x(1-x)y(1-y)$ . The aim is to use our adaptive strategy to choose  $\epsilon$  in such a way that the error from the penalty method is of the same order as the discretization error. Since the exact solution is known we first present a plot, Figure 1, with the energy semi-norm of the error calculated for different  $h$  (we use quasi-uniform meshes) and  $\epsilon$ . We see clearly for each  $h$  how the error eventually converges to the discretization error and we get no further improvement by decreasing  $\epsilon$ .

The adaptive strategy is designed to find the biggest  $\epsilon$  for which we achieve discretization error by considering the error estimators  $r_1$  and  $r_2$ . Figure 2 shows the values of the error estimators for a fix value of  $h = 0.025$ . We see that the discretization part of the error  $r_1$  is fairly constant and that the  $\epsilon$  dependent part  $r_2$  is proportional to  $\epsilon$ . It is clear that the two terms  $r_1$  and  $r_2$  captures the essence of the behavior of the error in the energy semi-norm. The adaptive strategy would in this situation suggest that  $\epsilon = \epsilon_0 r_1 / r_2$ . As seen when comparing the figures we get a slight over estimate of  $\epsilon$  arising from the fact that  $r_1$  is over estimated.

To sum up this example we analyze the  $h$ -dependence of  $\epsilon$  in our method. In this particular example  $\epsilon = \epsilon_0 r_1 / r_2$  for different  $\epsilon_0$  in the range  $10^{-1}$  to  $10^{-7}$ . As seen from the small clusters in Figure 3 we get very similar results on  $\epsilon$  for different  $\epsilon_0$ . We also recognize that  $\epsilon$  is proportional to  $h$ .

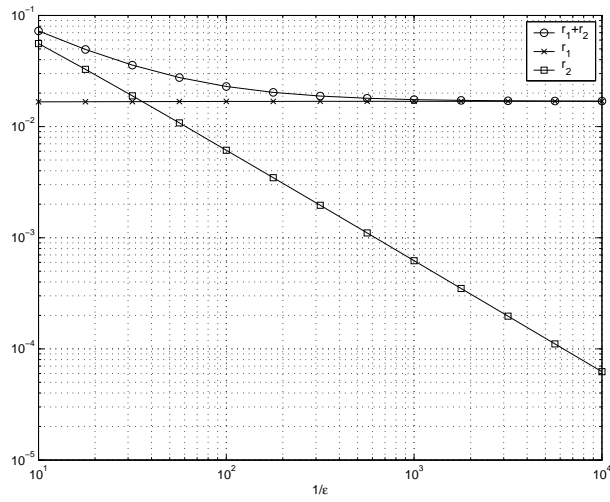


Figure 2: Error estimators dependence of  $\epsilon$ .

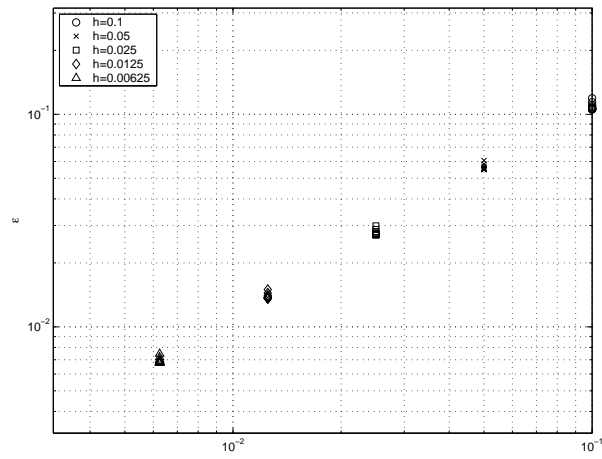


Figure 3: The penalty parameter  $\epsilon$  chosen according to adaptive strategy for different  $\epsilon_0$  and  $h$ .

777 nodes

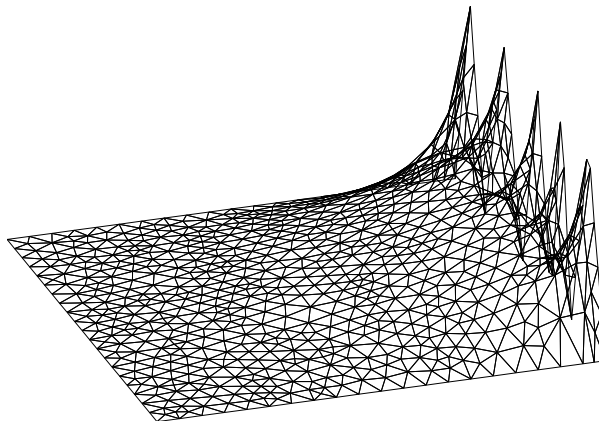


Figure 4: Solution to the second test problem

**Example 2.** Next we turn our attention to a situation where  $g \notin V$  on one part of the boundary. We let  $g = 0$  on three parts of the unit square and on the fourth part we let  $g$  be saw shaped as seen in Figure 4. The peaks and valleys are chosen so that they do not coincide with the mesh. Using a constant  $\epsilon$  would in this example not be the best approach since we need a very small  $\epsilon$  just on a part of the boundary where the normal derivative of the solution is large. Motivated by the results in Theorem 2.2 we use two different values of  $\epsilon$ ,  $\epsilon_1$  on the simple part and  $\epsilon_2$  on the complicated part. In Figure 5 we see the result of using our algorithm with  $\epsilon_0 = h$  as a starting guess for different  $h$ . The penalty parameter is chosen as

$$\epsilon_i = \epsilon_0 \frac{|\Gamma_i|}{|\Gamma|} \frac{\|hR(U)\|}{\|g - U\|_{1/2, \Gamma_i}}, \quad (4.1)$$

where  $|\Gamma_i|$  is the length of the boundary segment  $\Gamma_i$ . If the function  $g$  allows it can be convenient to replace  $\|g - U\|_{1/2, \Gamma}$  by  $\|g - U\|_{1, \Gamma}$  in practice. This gives a lower value of  $\epsilon$  but is simpler to compute. It is clear that the algorithm suggests us to choose a much higher  $\epsilon$  on the simple part of the domain. We also see that both  $\epsilon_1$  and  $\epsilon_2$  are proportional to  $h$  just with different constants.

**Example 3.** Finally we study an interesting effect that can arise from choosing  $\epsilon$  to small. From the earlier a priori work [3, 4] it is clear that this can lead to problems. This effect can not be seen explicitly from the a posteriori error estimates but it can be taken care of using the proposed adaptive strategy.

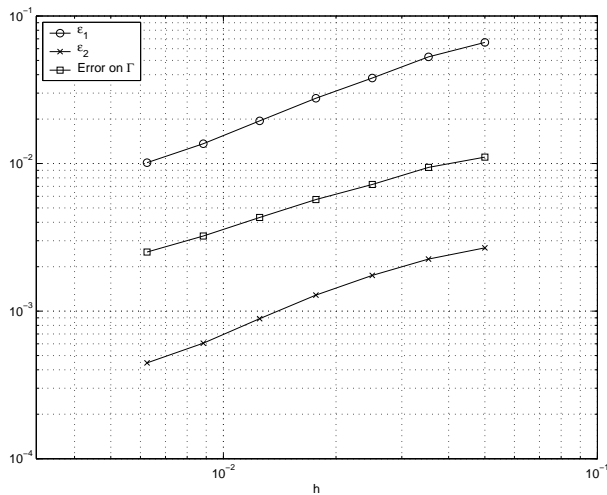


Figure 5: The boundary error  $\|e\|_{\Gamma}$  and  $\epsilon_i$  calculated for different values of  $h$ .

We let  $g$  be close to discontinuous, zero on one part of the boundary and one on the other with a very steep slope that connects the parts, see Figure 6. Further we let  $f = 1$ . We solve the problem by iterating the adaptive algorithm starting from  $\epsilon = h = 1/40$  and find an optimal  $\epsilon = 1/151$ , see Figure 6 (right). Then we solve the same problem using a ten times smaller  $\epsilon = 1/1510$  (left). We see clearly that a too small choice of  $\epsilon$  for this problem leads to oscillations in the solution. If  $\epsilon$  is decreased further the effect is even stronger.

The reason for this behavior is that equation (1.2) will force  $U \approx Pg$  if  $\epsilon$  is very small and it is known that the  $L^2$  projection  $P$  has oscillating behavior for discontinuous data. This example together with the size of the condition number motivates using the adaptive procedure when choosing  $\epsilon$ .

## 5 Conclusion

We have derived two a posteriori error estimates and designed an adaptive strategy for choosing the penalty parameter  $\epsilon$  in BPM for one of these. We present numerical examples that confirms our theoretical results and we conclude that by this strategy we achieve optimal order convergence for piecewise linear which agrees with earlier a priori work.

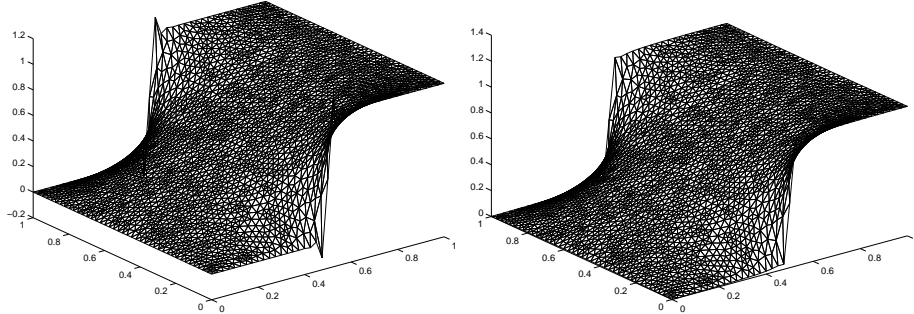


Figure 6: 10 times the optimal  $\epsilon$  to the left and optimal  $\epsilon$  to the right.

## References

- [1] R. A. Adams, *Sobolev spaces*, volume 65 of Pure and Applied Mathematics, Academic Press, New York, 1975.
- [2] I. Babuška, *The finite element method for elliptic equations with discontinuous solutions*, Computing, 5, 207-213, 1970.
- [3] I. Babuška, *The finite element method with penalty*, Mathematics of Computation, Volume 27, Number 122, 221-228, 1973.
- [4] J. W. Barrett and C. M. Elliott, *Finite element approximation of the Dirichlet problem using the boundary penalty method*, Numer. Math. 49, 343-366, 1986.
- [5] R. Becker, P. Hansbo, and Mats G. Larson, *Energy norm a posteriori error estimation for discontinuous Galerkin methods*, to appear in Comput. Methods Appl. Mech. Engrg.
- [6] S. C. Brenner and L. R. Scott, *The mathematical theory of finite element methods*, Springer Verlag, 1994.
- [7] C. Carstensen, *Merging the Bramble-Pasciak-Steinbach and the Crouzeix-Thomée criterion for the  $H^1$ -stability of the  $L^2$ -projection onto finite element spaces*, Math. Comp., 71, 237, 157-163, 2002.
- [8] C. Carstensen, S. Bartels, and S. Jansche *A posteriori error estimates for non-conforming finite element methods*, Mathematischen Seminars der Christian-Albrechts Universität zu Kiel Preprint 2000-13, 2000.

- [9] M. Crouzeix and V. Thomée, *The Stability in  $L_p$  and  $W_p^1$  of the  $L_2$ -projection onto Finite Element Function Spaces*, Mathematics of Computation, 48, 178, 521-532, 1987.
- [10] K. Eriksson, D. Estep, P. Hansbo and C. Johnson, *Computational differential equations*, Studentlitteratur, 1996.
- [11] V. Girault, P.-A. Raviart, *Finite element approximation of the Navier-Stokes equation*, Springer Verlag, Berlin, 1979.
- [12] A. Hansbo, P. Hansbo and Mats G. Larson, *A finite element method on composite grids based on Nitsches method*, preprint 2002.
- [13] M. G. Larson and A. J. Niklasson, *A posteriori error estimation of functionals in elliptic problems: experiments*, to appear in Math. Models Methods Appl. Sci.
- [14] R. D. Lazarov, J. E. Pasciak, J. Schöberl, and P. S. Vassilevski, *Almost optimal interior penalty discontinuous approximations of symmetric elliptic problems on non-matching grids*, Numer. Math., 96(2), 295-315, 2001.
- [15] J. Nitsche, *Über ein variationsprinzip für die lösung von Dirichlet problemen bei verwendung von teilräumen, die keinen randbedingungen unterworfen sind*, Abh. Math. Sem. Univ. Hamburg, v. 36, 1970/1971

# A Posteriori Error Analysis of Stabilized Finite Element Approximations of the Helmholtz Equation on Unstructured Grids

Mats G. Larson\*      Axel Målqvist†

April 7, 2004

## Abstract

In this paper we study the Galerkin least-squares method for minimizing pollution when solving Helmholtz equation. We especially consider how stochastic perturbations on a structured mesh affects the optimal choice of the method parameter  $\tau$ . The analysis is based on an error representation formula derived by a posteriori error estimates using duality. The primary goal with this work is not to present a brand new method for this problem but to show how existing methods derived for structured meshes can be modified to work on unstructured grids. We conclude that a parameter optimized for a structured mesh needs to be increased by a term proportional to the variance of the perturbation to be unbiased on a perturbed grid. We present numerical examples in one and two dimensions to confirm our theoretical results.

## 1 Introduction

It is well known that the standard Galerkin finite element method suffers from a substantial loss of accuracy when solving the Helmholtz equation for higher wave numbers. The problem is basically that the waves propagate too slow when using the standard Galerkin method. The solution is to increase the numerical wave number.

---

\*Corresponding author, Associate Professor, Department of Mathematics, Chalmers University of Technology, Göteborg, [mgl@math.chalmers.se](mailto:mgl@math.chalmers.se).

†Graduate Research Assistant, Department of Mathematics, Chalmers University of Technology, Göteborg, [axel@math.chalmers.se](mailto:axel@math.chalmers.se).

**Previous work.** The choice of numerical wave number have been solved by dispersion analysis in one and two dimension. In one dimension it is actually possible to achieve nodal exactness by the Galerkin Least-Squares (GLS) method, see [6, 9, 5], or the Generalized Finite Element Method (GFEM), see [2], and in two dimensions these methods gives significant improvement compared to the standard Galerkin method. The expression "pollution" is often used to describe this phenomenon and it was first stated in [2]. A draw back of using these methods to determine the numerical wave number in higher dimensions is that they are designed to be optimal for one certain direction on a structured grid.

Recent work on variational multiscale methods and subgrid modelling [8, 7] has given an understanding of the origin of GLS. It also represents an alternative to the dispersion analysis that works independent of the structure of the mesh. In a paper dealing with edge elements for electro-magnetic modelling [10] an improvement in accuracy when solving the vector Helmholtz equation was discovered on unstructured grids. This effect can also be seen in numerical studies for example in [5]. These results encouraged us to further investigate this area.

**New contributions.** Our goal with this paper is to understand how methods for minimizing pollution on structured grids needs to be modified to suit unstructured grids. To create the unstructured grid we start with a structured grid and add perturbations to the nodes from a given distribution. We need a method for computing an optimal method parameter  $\tau$  on a given mesh. We achieve this by deriving an error representation formula using a posteriori error estimation techniques iteratively and choosing  $\tau$  so this error functional equals zero. This method is independent of the structure of the mesh and converges to an optimal  $\tau$  in the sense that a given linear functional of the error is zero for this choice of  $\tau$ .

We then study a family of meshes with stochastic perturbations  $\delta_i$ , in each interior node  $i$ , and calculate the expected value of  $\tau$ ,  $E[\tau]$ . In one dimension we get the following result:

$$E[\tau] = Ch^2k^2(1 + 6\text{Var}(\delta_i)), \quad (1.1)$$

where  $C < 0$  is a constant that can be calibrated by a standard method on a structured grid e.g. see [5]. This means that the numerical wave number  $k_h$  modifies in the following way,  $k_h^2 = k^2(1 - \tau k^2)$ . From equation (1.1) we see clearly that the average of  $\tau$  calculated on perturbed grids will not be equal to  $\tau$  calculated on the structural grid. However we also see that for small perturbations,  $\tau$  from the structural calculation is a good estimate. The challenge is to extend this analysis to two dimensions where it is much harder to find an optimal  $\tau$ .

In two dimensions we again derive an optimal  $\tau$  independent of the structure of the mesh by using an error representation formula based on an a posteriori error estimate. The procedure needs to be done in an iterative fashion. A typical linear functional of the error we study could be an integral over the error over an outflow boundary. Again we recognize a modification of  $\tau$  proportional to the variance of the perturbation. For a plane wave in two dimensions numerical calculations shows improved results compared to a plane wave in one dimension. We argue that this effect arises from the fact that the variance of an integral of the error on the outflow boundary is smaller than the variance of the error measured in one point. This could explain the effect in [10].

Of course there are numerous advantages of using randomized unstructured meshes instead of structured ones. When it comes to wave propagation on of the most important are that a randomized mesh is isotropic i.e. "looks the same" in all directions. This means that if we can find an optimal  $\tau$  for one direction it will work well for waves propagating in an arbitrary direction.

**Outline** In §2 we present a one dimensional model problem, derive an a posteriori error estimate and state a formula for choosing the method parameter  $\tau$ . We then study how this choice of  $\tau$  depends on the structure of the mesh. In §3 we present numerical results for this problem and in §4 we turn our attention to a two dimensional model problem. Again we derive an a posteriori error estimate from which we can calculate the parameter  $\tau$ . In §5 we present numerical results for two test examples and finally in §6 we draw some conclusions of this work.

## 2 One Dimensional Model Problem

We consider the following one dimensional model problem: find  $u$  such that

$$\begin{cases} -u'' - k^2 u = 0 & \text{in } \Omega, \\ u'(0) = ik, \\ u'(\pi) = ik u(\pi), \end{cases} \quad (2.1)$$

where  $\Omega = [0, \pi]$ . This setting makes the wave propagate freely from left to right with analytic solution  $u(x) = e^{ikx}$ . The corresponding weak formulation reads: find  $u \in H^1(\Omega)$  such that

$$(u', v') - k^2 (u, v) - ik u(\pi)v(\pi)^* = -ik v(0)^*, \quad \text{for all } v \in H^1(\Omega), \quad (2.2)$$

where  $(\cdot, \cdot)$  is the ordinary  $L^2(\Omega)$  scalar product and  $v(x)^*$  is the complex conjugate of  $v(x)$ .

## 2.1 The Galerkin Least-Squares Method

The GLS stabilization, see [6], of the weak form reads: find  $u \in H^1(\Omega)$  such that

$$(u', v') - k^2 (u, v) + (\tau Lu, Lv)_{\tilde{\Omega}} - ik u(\pi)v(\pi)^* = -ik v(0)^*, \quad \text{for all } v \in H^1(\Omega), \quad (2.3)$$

where  $\tau$  is a complex number,  $L = -\frac{\partial^2}{\partial x^2} - k^2$ , and  $\tilde{\Omega}$  is the union of element interiors. This method can now be discretized and we can introduce  $p = 1 - \tau k^2$  as the new parameter. If we for the sake of simplicity only consider the space  $V$  of piecewise linear base functions we get: find  $U \in V$  such that

$$(U', v') - k^2 p (U, v) - ik U(\pi)v(\pi)^* = -ik v(0)^*, \quad \text{for all } v \in V. \quad (2.4)$$

Here we see that the stabilization is done basically by changing the wave number in the Galerkin method, see [6]. Next we present an a posteriori error analysis for the piecewise linear case.

## 2.2 Error Representation Formula

We would like to choose  $p$  in order to minimize a given linear functional of the error  $e = u - U$  i.e.  $(e, \psi)$ , where  $\psi$  is a given function in  $H^{-1}(\Omega)$ . We begin the a posteriori analysis by presenting the dual problem: find  $\phi$  such that

$$\begin{cases} -\phi'' - k^2 \phi = \psi & \text{in } \Omega, \\ \phi'(0) = 0, \\ \phi'(\pi) = -ik \phi(\pi), \end{cases} \quad (2.5)$$

We proceed with the following calculation,

$$(e, \psi) = (e, -\phi'' - k^2 \phi) \quad (2.6)$$

$$= (e', \phi') - (k^2 e, \phi) - [e\phi'^*]_0^\pi \quad (2.7)$$

$$= -(U', \phi') + (k^2 U, \phi) + [u' \phi^*]_0^\pi - ik e(\pi)\phi(\pi)^* \quad (2.8)$$

$$= (U'', \phi - \pi\phi) + (k^2 U, \phi - \pi\phi) - (U', \pi\phi) \quad (2.9)$$

$$+ (k^2 U, \pi\phi) + ik U(\pi)\phi(\pi)^* - ik \phi(0)^*$$

$$= (U'', \phi - \pi\phi) + (k^2 U, \phi - \pi\phi) + (\tau k^4 U, \pi\phi) \quad (2.10)$$

$$= (k^2 U, \phi - \pi\phi) + (\tau k^4 U, \pi\phi). \quad (2.11)$$

This calculation suggests that  $\tau = -\frac{(k^2 U, \phi - \pi\phi)}{(k^4 U, \pi\phi)}$  or in terms of  $p$ ,

$$\boxed{p = 1 - \tau k^2 = \frac{(U, \phi)}{(U, \pi\phi)}} \quad (2.12)$$

would make  $(e, \psi)$  small.

**Remark 2.1** We also note that if there exists a  $\hat{\tau}$  such that  $(e, \psi) = 0$  it can always be written on the form  $\hat{\tau} = -\frac{(k^2 U, \phi - \pi\phi)}{(k^4 U, \pi\phi)}$  or  $\hat{p} = \frac{(U, \phi)}{(U, \pi\phi)}$ .

**Remark 2.2** In practice  $\phi$  will not be known so we have to calculate it numerically. Since we need to subtract the interpolant we use higher order elements for the dual problem. However this is a computationally expensive way of getting high accuracy and should primarily be used if error control is essential.

It is possible to proceed iteratively starting with  $p_0 = 1$  solving equation (2.4) for  $U_n$  and choosing,

$$p_{n+1} = \frac{(U_n, \phi)}{(U_n, \pi\phi)} \quad \text{for } n = 0, 1, \dots \quad (2.13)$$

In section 3 we present numerical results that shows fast convergence for this particular algorithm for nodal error control. We are going to use the iterative algorithm described in equation (2.13) to calculate optimal values of  $p$  on perturbed grids. In this way we can study how an optimal  $p$  depends on the size of the perturbation  $\delta$ .

### 2.3 Unstructured Mesh

We introduce a new parameter  $0 \leq \delta < 1$  which is a measure of how unstructured the mesh is. We divide  $[0, \pi]$  into  $n$  subintervals in the following way,

$$\begin{cases} x_0 &= 0 \\ x_i &= \frac{i\pi}{n} + \delta_i, \quad \text{for } i = 1, \dots, n-1, \\ x_n &= \pi, \end{cases}$$

where  $\delta_i \in U(-\frac{\delta\pi}{2n}, \frac{\delta\pi}{2n})$ , see Figure 1. From this definition we note that the interval length  $h_i = x_i - x_{i-1}$  the perturbed mesh is equal to  $h + \delta_i - \delta_{i-1}$ . With this notation we need to define  $\delta_0 = \delta_n = 0$ . We are interested in how the expected value and the variance of the error  $(e, \psi)$  depends on  $\delta$ ,  $h = \pi/n$ , and  $k$ . We now see  $p$  as a stochastic parameter  $\hat{p}$  and use equation (2.11) to get,

$$(e, \psi) = k^2(U, \phi - \pi\phi) - k^2(\hat{p} - 1)(U, \pi\phi). \quad (2.14)$$

Our aim is to find  $p = E[\hat{p}]$  such that  $E[(e, \psi)] = 0$  for a given  $\delta$ . We start with the following Lemma.

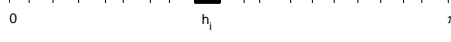


Figure 1: One dimensional unstructured mesh with  $n = 19$  and  $\delta = 0.4$ .

**Lemma 2.1** *Let  $z \in C^2([0, h])$  such that  $z(0) = z(h) = 0$ ,  $\varphi_0 = 1 - \frac{x}{h}$ , and  $\varphi_1 = \frac{x}{h}$ . Then we have,*

$$\begin{aligned} \int_0^h \varphi_0 z dx &= -\frac{h^2}{3} \int_0^h \varphi_0^2 \varphi_1 z'' dx - \frac{h^2}{6} \int_0^h \varphi_0 \varphi_1^2 z'' dx, \\ \int_0^h \varphi_1 z dx &= -\frac{h^2}{6} \int_0^h \varphi_0^2 \varphi_1 z'' dx - \frac{h^2}{3} \int_0^h \varphi_0 \varphi_1^2 z'' dx. \end{aligned} \quad (2.15)$$

**Proof.** We start with  $\int_0^h \varphi_i z dx$  for  $i = 0, 1$  and integrate by part. We use the fact that  $(-h\varphi_0)' = 1$ ,  $(h\varphi_1)' = 1$  and that the boundary term will vanish since  $z(0) = z(h) = 0$  to get,

$$\begin{aligned} \int_0^h \varphi_0 z dx &= \frac{h}{2} \int_0^h \varphi_0^2 z' dx, \\ \int_0^h \varphi_1 z dx &= -\frac{h}{2} \int_1^h \varphi_1^2 z' dx. \end{aligned} \quad (2.16)$$

Next we proceed with the first equation in (2.16) and use that  $(h\varphi_1)' = 1$  and integrate by parts,

$$\int_0^h \varphi_0^2 z' dx = -h \int_0^h \varphi_1 (\varphi_0^2 z')' dx = 2 \int_0^h \varphi_0 \varphi_1 z' dx - h \int_0^h \varphi_1 \varphi_0^2 z'' dx. \quad (2.17)$$

Since  $\varphi_0 + \varphi_1 = 1$  on  $[0, h]$  we have,

$$0 = \int_0^h (\varphi_0 + \varphi_1)^2 z' dx = \int_0^h (\varphi_0^2 + 2\varphi_0 \varphi_1 + \varphi_1^2) z' dx, \quad (2.18)$$

inserted in equation (2.17) this yields

$$\int_0^h \varphi_0^2 z' dx = -\frac{1}{2} \int_0^h \varphi_1^2 z' dx - \frac{h}{2} \int_0^h \varphi_0^2 \varphi_1 z'' dx. \quad (2.19)$$

A similar calculation gives

$$\int_0^h \varphi_1^2 z' dx = -\frac{1}{2} \int_0^h \varphi_0^2 z' dx - \frac{h}{2} \int_0^h \varphi_0 \varphi_1^2 z'' dx. \quad (2.20)$$

Together equation (2.19) and equation (2.20) now gives

$$\begin{aligned} \int_0^h \varphi_0^2 z' dx &= -\frac{2h}{3} \int_0^h \varphi_0^2 \varphi_1 z'' dx - \frac{h}{3} \int_0^h \varphi_0 \varphi_1^2 z'' dx, \\ \int_0^h \varphi_1^2 z' dx &= \frac{h}{3} \int_0^h \varphi_0^2 \varphi_1 z'' dx + \frac{2h}{3} \int_0^h \varphi_0 \varphi_1^2 z'' dx. \end{aligned} \quad (2.21)$$

Finally we combine equation (2.16) and (2.21) to prove the Lemma.  $\square$

We initially need to study how the first term in equation (2.14) depends on the stochastic parameters  $\{\delta_i\}_{i=1}^{n-1}$ .

$$(U, \phi - \pi\phi) = \sum_{i=1}^n \int_{x_{i-1}}^{x_i} U(\phi - \pi\phi) dx \quad (2.22)$$

On each element  $[x_{i-1}, x_i]$  we assume  $\phi \in C^2([x_{i-1}, x_i])$  and apply Lemma 2.1 with  $z = \phi - \pi\phi$ ,  $\varphi_0 = \varphi_{i-1}$ ,  $\varphi_1 = \varphi_i$ , and  $h = h_i$  to get,

$$(U, \phi - \pi\phi) = \sum_{i=1}^n \int_{x_{i-1}}^{x_i} U(\phi - \pi\phi) dx \quad (2.23)$$

$$= \sum_{i=1}^n U_{i-1} \int_{x_{i-1}}^{x_i} \varphi_{i-1}(\phi - \pi\phi)(x) dx \quad (2.24)$$

$$+ \sum_{i=1}^n U_i \int_{x_{i-1}}^{x_i} \varphi_i(\phi - \pi\phi)(x) dx$$

$$= - \sum_{i=1}^n \frac{h_i^2}{6} \int_{x_{i-1}}^{x_i} \phi'' \varphi_{i-1} \varphi_i (U(x) + U_{i-1} + U_i) dx \quad (2.25)$$

$$= - \sum_{i=1}^n h_i^3 \frac{1}{h_i} \int_{x_{i-1}}^{x_i} \frac{1}{6} \phi'' \varphi_{i-1} \varphi_i (U(x) + U_{i-1} + U_i) dx. \quad (2.26)$$

We introduce the following notation,

$$z_i(\{\delta_i\}_{i=1}^{n-1}) = - \frac{k^2}{h_i} \int_{x_{i-1}}^{x_i} \frac{1}{6} \phi'' \varphi_{i-1} \varphi_i (U(x) + U_{i-1} + U_i) dx. \quad (2.27)$$

With this notation equation (2.14) and equation (2.23) now gives

$$(e, \psi) = \sum_{i=1}^n h_i^3 z_i - (\hat{p} - 1) \int_0^\pi k^2 U \pi \phi dx. \quad (2.28)$$

We now make the following simplification. We replace  $z_i$  in equation (2.28) with  $\bar{z}_i$  which is  $z_i$  calculated on a structured grid i.e.

$$\bar{z}_i = - \frac{k^2}{h} \int_{(i-1)h}^{ih} \frac{1}{6} \phi'' \bar{\varphi}_{i-1} \bar{\varphi}_i (\bar{U}(x) + \bar{U}_{i-1} + \bar{U}_i) dx, \quad (2.29)$$

where  $\bar{\varphi}_i$  are the base functions on the structured grid and  $\bar{U}$  is the solution on the structured grid. This means that  $\bar{z}_i$  are not stochastic variables.

We also introduce  $\bar{w} = \int_0^\pi k^2 \bar{\pi} \phi(x) \bar{U}(x) dx$ , where  $\bar{\pi}$  is the Scott-Zhang interpolant, see [3], onto the structured grid, i.e  $\bar{w}$  is not stochastic.

If  $hk$  is small these approximations can be motivated by linearization in terms of  $\delta$  but the most important argument is the good agreement we get with numerical experiments, see section 3. We define an approximation to  $(e, \psi)$  in the following way,

$$\bar{e}_\psi = \sum_{i=1}^n h_i^3 \bar{z}_i - (\hat{p} - 1) \bar{w}, \quad (2.30)$$

and we choose  $\hat{p}$  such that  $\bar{e}_\psi = 0$  i.e.

$$\hat{p} = 1 + \frac{1}{\bar{w}} \sum_{i=1}^n h_i^3 \bar{z}_i. \quad (2.31)$$

Since we want to find one parameter  $p$  that suits many meshes with a given  $\delta$  we study the expected value of  $\hat{p}$ . To do this we need to do the following observation,

$$E[\hat{p}] = 1 + \frac{1}{\bar{w}} E \left[ \sum_{i=1}^n h_i^3 \bar{z}_i \right] \quad (2.32)$$

$$= 1 + \frac{1}{\bar{w}} \sum_{i=1}^n E[h_i^3] \bar{z}_i \quad (2.33)$$

$$= 1 + \frac{1}{\bar{w}} \sum_{i=1}^n E[(h + \delta_i - \delta_{i-1})^3] \bar{z}_i \quad (2.34)$$

$$= 1 + \frac{1}{\bar{w}} \sum_{i=1}^n E[h^3 + 3h^2(\delta_i - \delta_{i-1}) + 3h(\delta_i - \delta_{i-1})^2 + (\delta_i - \delta_{i-1})^3] \bar{z}_i \quad (2.35)$$

$$= 1 + \frac{1}{\bar{w}} \sum_{i=1}^n (h^3 + 3h^2 E[\delta_i - \delta_{i-1}]) \bar{z}_i \quad (2.36)$$

$$+ \frac{1}{\bar{w}} \sum_{i=1}^n (3h E[(\delta_i - \delta_{i-1})^2] + E[(\delta_i - \delta_{i-1})^3]) \bar{z}_i$$

$$= 1 + \frac{1}{\bar{w}} \sum_{i=1}^n (h^3 + 3h E[(\delta_i - \delta_{i-1})^2]) \bar{z}_i \quad (2.37)$$

$$= 1 + \frac{1}{\bar{w}} \sum_{i=1}^n (h^3 + 6h \text{Var}(\delta_i)) \bar{z}_i \quad (2.38)$$

$$= 1 + \frac{\sum_{i=1}^n h \bar{z}_i}{\bar{w}} (h^2 + 6 \text{Var}(\delta_i)), \quad (2.39)$$

where we use that  $\{\delta_i\}_{i=1}^{n-1}$  are independent,  $E[\delta_i] = 0$ , and  $E[\delta_i^2] = E[\delta_{i-1}^2] = \text{Var}(\delta_i)$ . We neglect the boundary effect due to the fact that  $\delta_0$  and  $\delta_n$  are not stochastic. If we let  $\bar{z} = \sum_{i=1}^n h\bar{z}_i$  we have

$$\boxed{p = E[\hat{p}] = 1 + \frac{\bar{z}}{\bar{w}}(h^2 + 6\text{Var}(\delta_i))} \quad (2.40)$$

**Remark 2.3** For the uniform distribution  $\text{Var}(\delta_i) = \frac{h^2\delta^2}{12}$  i.e.

$$p = 1 + \frac{\bar{z}}{\bar{w}}h^2 \left(1 + \frac{\delta^2}{2}\right) \quad (2.41)$$

**Remark 2.4** Given  $\delta$  we can find  $p$  by using one for the standard methods [5, 2] for structured meshes and then add the contribution suggested in equation (2.41). For example if we want nodal exactness in the right endpoint  $x = \pi$  we can use the formula from [5] for nodal exactness on structured mesh to find  $\bar{z}/\bar{w}$ .

Given a formula (2.41) to find  $p$  we would like to estimate the error  $(e, \psi)$  in terms of  $h$ ,  $k$ , and  $\delta$ . We start by estimating the variance of  $\bar{e}_\psi$ .

**Proposition 2.1** *It holds*

$$\text{Var}(\bar{e}_\psi) = h^6 \left( \frac{3}{2}\delta^2 + \frac{3}{4}\delta^4 + \frac{1}{28}\delta^6 \right) \sum_{i=1}^n \bar{z}_i^2 \quad (2.42)$$

**Proof.** We start from equation (2.30) with  $\hat{p}$  chosen according to equation

(2.32). We note that  $E[\bar{e}_\psi] = 0$  so  $\text{Var}(\bar{e}_\psi) = E[\bar{e}_\psi^2]$ ,

$$\text{Var}(\bar{e}_\psi) = E[\bar{e}_\psi^2] \quad (2.43)$$

$$= E \left[ \left( \sum_{i=1}^n h_i^3 \bar{z}_i - (\hat{p} - 1)\bar{w} \right)^2 \right] \quad (2.44)$$

$$= E \left[ \left( \sum_{i=1}^n h_i^3 \bar{z}_i \right)^2 \right] - 2E \left[ \sum_{i=1}^n h_i^3 \bar{z}_i \right] E[(\hat{p} - 1)\bar{w}] + E[(\hat{p} - 1)\bar{w}]^2 \quad (2.45)$$

$$= E \left[ \left( \sum_{i=1}^n h_i^3 \bar{z}_i \right)^2 \right] - 2E \left[ \sum_{i=1}^n h_i^3 \bar{z}_i \right] E \left[ \sum_{i=1}^n h_i^3 \bar{z}_i \right] + E \left[ \sum_{i=1}^n h_i^3 \bar{z}_i \right]^2 \quad (2.46)$$

$$= E \left[ \left( \sum_{i=1}^n h_i^3 \bar{z}_i \right)^2 \right] - E \left[ \sum_{i=1}^n h_i^3 \bar{z}_i \right]^2 \quad (2.47)$$

$$= \sum_{i=1}^n (E[h_i^6] - E[h_i^3]^2) \bar{z}_i^2. \quad (2.48)$$

We need to calculate the expected value of different powers of  $\delta_i$ . We have  $E[\delta_i^{2n-1}] = 0$  and

$$E[\delta_i^{2n}] = \frac{\delta^{2n} h^{2n}}{(2n+1)2^{2n}}, \quad (2.49)$$

for all  $n \in \mathbf{N}$ . We use these result and  $h_i = h + \delta_i - \delta_{i-1}$  to get,

$$\text{Var}(\bar{e}_\psi) = \sum_{i=1}^n (E[h_i^6] - E[h_i^3]^2) \bar{z}_i^2 \quad (2.50)$$

$$= \sum_{i=1}^n h^6 \left( 1 + \frac{5}{2}\delta^2 + \delta^4 + \frac{1}{28}\delta^6 - 1 - \delta^2 - \frac{1}{4}\delta^4 \right) \bar{z}_i^2 \quad (2.51)$$

$$= \sum_{i=1}^n h^6 \left( \frac{3}{2}\delta^2 + \frac{3}{4}\delta^4 + \frac{1}{28}\delta^6 \right) \bar{z}_i^2, \quad (2.52)$$

which proves the proposition.  $\square$

We need to estimate the sum in equation (2.42) in terms of  $h$  and  $k$ . For  $\psi \in H^{-1}(\Omega)$  independent of  $h$  and  $k$  we have  $|\phi| \leq C/k$  for some constant  $C$  and thereby  $|\phi''| \leq Ck$ . The magnitude of the numeric solution  $U$  is

independent of  $k$  so from equation (2.27) we get  $|\bar{z}_i| \leq Ck^3$ . This yields

$$\sum_{i=1}^n \bar{z}_i^2 \leq \sum_{i=1}^n Ck^6 \leq C \frac{k^6}{h}. \quad (2.53)$$

We are not interested in tracking the constants in the following theory, only the  $h$ ,  $k$ , and  $\delta$  dependence. If we neglect the  $\delta^4$  and  $\delta^6$  terms in Proposition 2.1 and use it together with equation (2.53) we get

$$\text{Var}(\bar{e}_\psi) \leq Ch^5 k^6 \delta^2. \quad (2.54)$$

Since  $E[\bar{e}_\psi] = 0$  we can use the Chebyshev inequality to get a bound of  $|\bar{e}_\psi|$ ,

$$P(|\bar{e}_\psi| > \epsilon) \leq \frac{\text{Var}(\bar{e}_\psi)}{\epsilon^2}. \quad (2.55)$$

By choosing  $\epsilon = D\delta h^{5/2} k^3$  we get  $P(|\bar{e}_\psi| > D\delta h^{5/2} k^3) \leq \frac{C}{D}$  hence with  $D$  large we can make this quantity arbitrarily small i.e. there exists  $C$  independent of  $\delta$ ,  $h$ , and  $k$  such that

$$\boxed{P(|\bar{e}_\psi| \leq C\delta h^{5/2} k^3) > 1 - \epsilon} \quad (2.56)$$

for each  $\epsilon > 0$ .

### 3 Numerical Results in One Dimension

We study pointwise error control. This is done by choosing  $\psi$  as the Dirac delta measure in a chosen node. We can actually find an analytic formula for the dual solution in this case,

$$\phi_z(x) = \frac{e^{ik(\pi-z)}}{ik\epsilon^{ik\pi}} \cos(kx) - \frac{1}{k} \sin(k(x-z)) I_{\{x>z\}}, \quad (3.1)$$

where  $z$  indicates a point mass in  $x = z$ . We note that  $\phi_z(x) \in C^2([x_{i-1}, x_i])$  for  $i = 1, \dots, n$ . We proceed with a numerical simulation to verify that the iterative algorithm described in equation (2.13) converges and gives an optimal value of  $p$ . Figure 2 shows rapid convergence for the iterative algorithm towards machine precision. Here  $\psi$  is chosen as the dirac measure in  $x = \pi$  i.e.  $\psi = \delta_\pi$ .

In Figure 3 we illustrate how well equation (2.41), where  $\bar{z}/\bar{w}$  is calculated on a structured mesh, compares to numerical experiments of the iterative a posteriori method, equation (2.13). For each  $\delta$ , 5000 meshes have been evaluated, by iteration until convergence, and the stars are the mean value of these. The dashed line is the theoretical value of equation

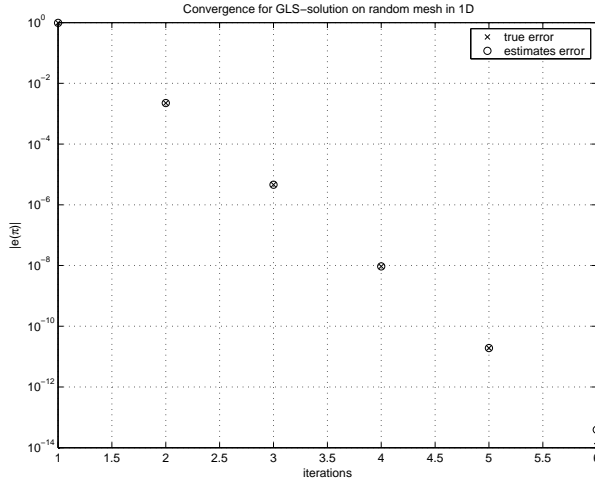


Figure 2: The error  $|u(\pi) - U(\pi)|$  versus number of iterations

(2.41). We see quite a good agreement between numerics and theory. Remember that the theoretical value is based on approximations. The variance is proportional to the square of  $\delta$  which agree with the theoretical result in equation (2.41).

By changing  $h$  and  $k$  separately while holding  $\delta = 0.1$  we also get an idea of how the variance of  $\hat{p}$  depends on these variables, see Figure 4. In this particular case we get  $\text{Var}(\hat{p}) \sim h^{7.3}k^{6.1}$  or  $\text{Var}((e, \psi)) \sim h^{7.3}k^{8.1}$ , since  $\text{Var}((e, \psi)) \sim k^4(U, \pi\phi)^2\text{Var}(p) \sim k^2\text{Var}(p)$ , which is even better than  $\text{Var}(\bar{e}_\psi) \leq Ch^5k^6$  that we got from theory, see equation (2.54).

Another interesting measure of the error is the mean value i.e.  $\psi = 1$ . Letting  $v = 1$  in (2.4) gives us,  $(U, 1) = \frac{i}{kp}(1 - U(\pi))$ . We have  $u = e^{ikx}$  so  $(u, 1) = \frac{i(1-u(\pi))}{k}$  which makes

$$(e, 1) = -\frac{i}{kp}e(\pi) + \frac{(p-1)}{p}(u, 1). \quad (3.2)$$

Since  $p$  is close to one this calculation shows that the nodal error in  $\pi$  is very closely related to the mean of the error and coincides if  $k = 2n$ ,  $n \in \mathbf{N}$ , since  $(u, 1) = 0$  in that case.

## 4 Two Dimensional Model Problem

In two dimensions we consider a plane wave with wave number

$$\mathbf{k} = k(\cos(\theta), \sin(\theta)) \quad (4.1)$$

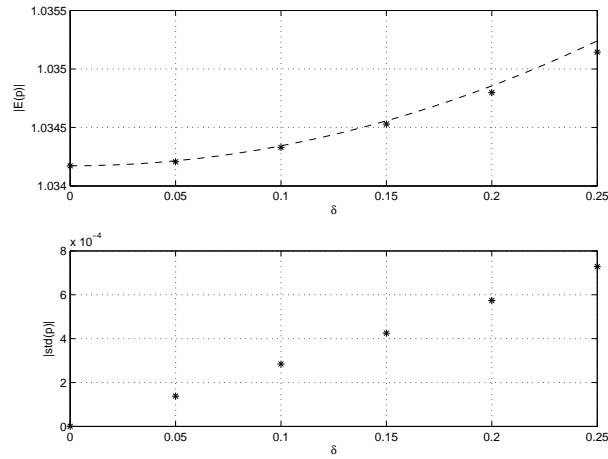


Figure 3: The expected value,  $|E[\hat{p}]|$  (above), and the standard deviation,  $|\sigma(\hat{p})|$  (below), verses  $\delta$ .

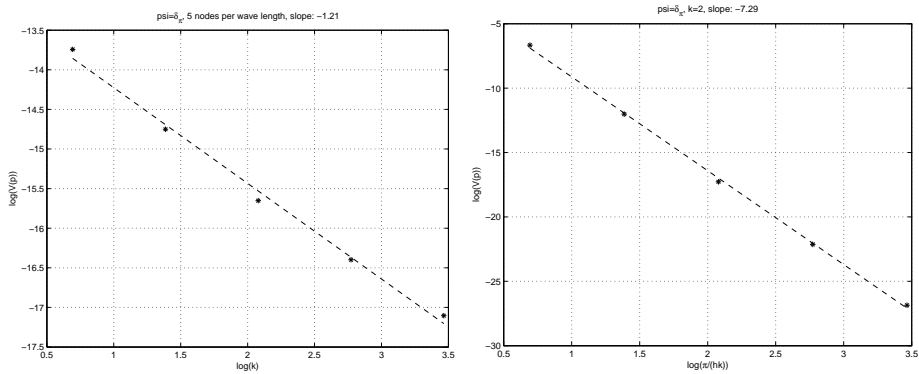


Figure 4:  $\log(\text{Var}(\hat{p}))$  versus  $\log k$  (left) and the logarithm of the number of nodes per wavelength (right).

propagating on a unit square, see Figure 5. We use a model problem from [5] with inhomogeneous Robin boundary conditions chosen such that the solution  $u$  is equal to  $e^{ik \cdot x}$ : find  $u \in H^1(\Omega)$  such that

$$\begin{cases} -\Delta u - k^2 u = 0 & \text{in } \Omega, \\ -\partial_n u = -ik(u - g) & \text{on } \Gamma, \end{cases} \quad (4.2)$$

where  $\Omega$  is a polygonal domain in  $\mathbf{R}^d$ ,  $d = 2, 3$  with boundary  $\Gamma$ .

#### 4.1 The Galerkin Least-Squares Method

The corresponding discretized GLS method reads: find  $U \in V \subset H^1(\Omega)$  such that

$$(\nabla U, \nabla v) - k^2 (U, v) + (\tau LU, Lv)_{\tilde{\Omega}} - ik(U, v)_{\Gamma} = -ik(g, v)_{\Gamma}, \quad \text{for all } v \in V, \quad (4.3)$$

where  $(\cdot, \cdot)_{\Gamma}$  is the  $L^2(\Gamma)$  scalar product,  $L = -\Delta - k^2$  and  $V$  is the finite element space of piecewise polynomials of degree  $p$ . Again we want to find a criteria for choosing  $\tau$  that minimizes a given linear functional of the error. We proceed as in the one dimensional case starting with the error representation formula.

#### 4.2 Error Representation Formula

The corresponding dual problem reads: find  $\phi$  such that

$$\begin{cases} -\Delta \phi - k^2 \phi = \psi_{\Omega} & \text{in } \Omega, \\ -\partial_n \phi = ik(\phi - \psi_{\Gamma}) & \text{on } \Gamma, \end{cases} \quad (4.4)$$

where  $\psi_{\Omega} \in H^{-1}(\Omega)$  and  $\psi_{\Gamma} \in H^{1/2}(\Gamma)$ , see [1] for a definition of these spaces. To the right in Figure 5 we have the dual solution calculated for  $\psi$  as a point mass in  $(0.5, 0.5)$ . In this setting we consider two types of linear functionals of the error at the same time, namely  $(e, \psi_{\Omega})$  and  $(e, \psi_{\Gamma})_{\Gamma}$ . The a posteriori analysis gives,

$$(e, \psi_{\Omega}) - ik(e, \psi_{\Gamma})_{\Gamma} = (\nabla e, \nabla \phi) - (k^2 e, \phi) + (e, ik\phi)_{\Gamma} \quad (4.5)$$

$$= (\partial_n u, \phi)_{\Gamma} - (\nabla U, \nabla \phi) + (k^2 U, \phi) + (e, ik\phi)_{\Gamma} \quad (4.6)$$

$$= (ik(U - g), \phi)_{\Gamma} - (\nabla U, \nabla \phi - \pi\phi) + (k^2 U, \phi - \pi\phi) \quad (4.7)$$

$$\begin{aligned} & - (\nabla U, \nabla \pi\phi) + (k^2 U, \pi\phi) \\ & = (\Delta U + k^2 U, \phi - \pi\phi) - (\partial_n U - ik(U - g), \phi - \pi\phi)_{\Gamma} \end{aligned} \quad (4.8)$$

$$+ (\tau LU, L\pi\phi)_{\tilde{\Omega}},$$

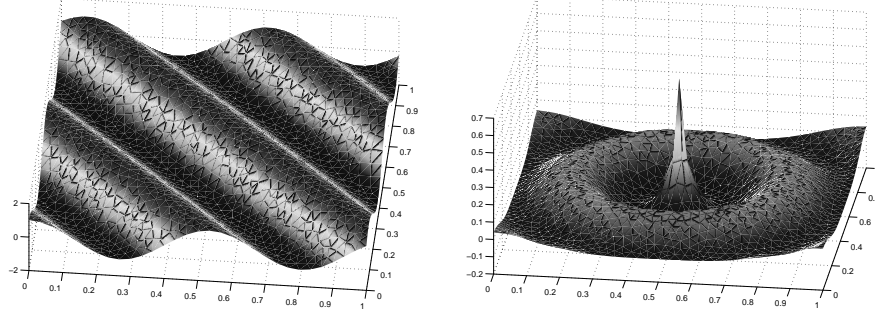


Figure 5: Real part of the solution to the primal problem with  $\theta = \pi/4$  and to the dual problem with  $\psi_\Omega = \delta_{[.5,.5]}$

where the first scalar product in the last row is defined in the following way,

$$(\Delta U, v) = \sum_{K \in \mathcal{K}} \int_K \Delta U v \, dx - \sum_{K \in \mathcal{K}} \int_{\partial K \setminus \Gamma} \frac{\partial U}{\partial n_K} v \, ds, \quad \text{for all } v \in H^1(\Omega), \quad (4.9)$$

where  $K$  refers to elements in the mesh with boundary  $\partial K$  and  $\mathcal{K} = \{K\}$  is the set of elements in the mesh. We get the following error representation formula,

$$(e, \psi_\Omega) - ik(e, \psi_\Gamma)_\Gamma = (-LU, \phi - \pi\phi) + (-\partial_n U + ik(U - g), \phi - \pi\phi)_\Gamma + (\tau LU, L\pi\phi)_{\tilde{\Omega}}. \quad (4.10)$$

We derive a method for choosing  $\tau$  by letting (4.10) be equal to zero,

$$\tau = - \frac{(\Delta U + k^2 U, \phi - \pi\phi) - (\partial_n U - ik(U - g), \phi - \pi\phi)_\Gamma}{(LU, L\pi\phi)_{\tilde{\Omega}}} \quad (4.11)$$

We define  $(R_\Omega, v) = (\Delta U + k^2 U, v)$ , for all  $v \in H^1(\Omega)$ , and  $(R_\Gamma, v)_\Gamma = (\partial_n U + ik(U - g), v)_\Gamma$ , for all  $v \in H^1(\Gamma)$ , as domain and boundary residual.

Again we end up with a strategy for choosing  $\tau$ . As in the one-dimensional case this approach is independent of the structure of the mesh. We consider plane waves sent in different angles over the unit square. The one dimensional analysis suggests that there exists a parameter that gives us a good approximation if  $\delta$  as a function of  $\theta$  is close to constant. This is the case on a totally unstructured mesh but can never be the case for a structured mesh. This implies that we only need to optimize for one angle  $\theta$  by the method described in equation (4.11) to get a good approximation for all angles. The reason for this is that a totally unstructured is much more isotropic than a structured mesh (if the domain is large enough).

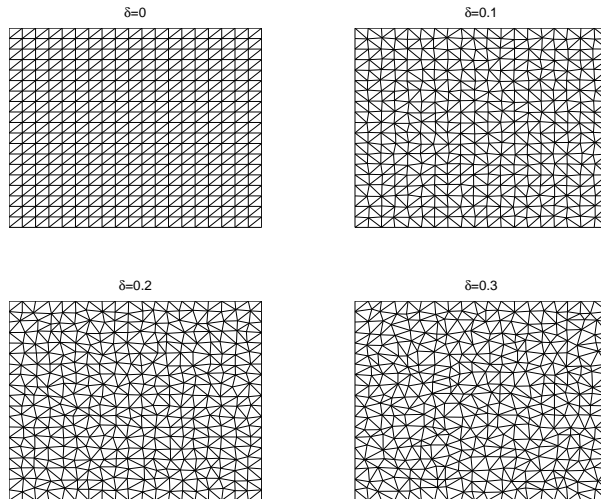


Figure 6: Delaunay triangulations with various  $\delta$ .

## 5 Numerical Results in Two Dimensions

We study problems on two different geometries.

**Example 1.** First we study a plane wave on the unit square. We use the same setting as in [5] i.e. Robin type boundary conditions that approximately makes the wave propagate freely over the boundaries. Since we are interested in calculating a correction for unstructured meshes and also how this correction compares to earlier work on structured grids we start with a regular mesh constructed by the Delaunay algorithm on a two dimensional lattice. Then we add small perturbations to the interior nodes and proceed with another Delaunay triangulation, see Figure 6. We introduce a parameter  $\delta$  in analogy with the one dimensional case that measure how unstructured the mesh is. Now the perturbation of the interior nodes are done both in  $x$  and  $y$  direction so  $\delta$  has two entries  $(\delta_x, \delta_y)$ . Below  $\delta_x = \delta_y = \delta$  if nothing else is mentioned. On these meshes we calculate an optimal  $p$  for error control on the outflow boundary  $\Gamma_o$  when the wave propagates in the  $x$ -direction i.e.  $\theta = 0$ . This means that  $\Gamma_o = \{(x, y) : x = 1, 0 \leq y \leq 1\}$ . In equation (4.10) this is achieved by letting  $\psi_\Omega = 0$  and  $\psi_\Gamma = I_{\Gamma_o}$  to get  $\phi$  and then using equation (4.11). To get small error i.e. find the optimal  $p$  we repeat this process iteratively in analogy with equation (2.13) until the error is about one millionth of the Galerkin error.

In Figure 7 we see how  $p$  depends on  $\delta$ . It is slowly increasing for small  $\delta$

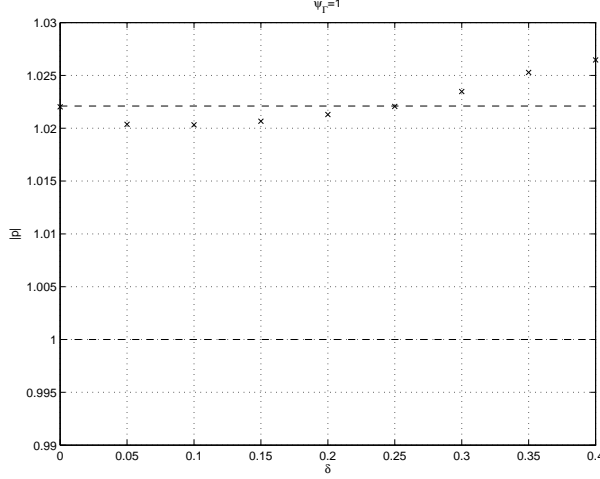


Figure 7:  $p$  optimized for error control with  $\psi_\Omega = 0$  and  $\psi_\Gamma = I_{\Gamma_o}$  on various unstructured meshes.

except a jump between  $\delta = 0$  and  $\delta = 0.05$  depending on the big structural change in the grid. For  $\delta = 0$  we have a regular mesh and for  $\delta = 0.05$  we get an approximate union jack shape. For bigger  $\delta$  we see that  $p$  increases in the same way as in the the one dimensional case. The dashed lines are from a classic GLS-method optimized for the regular mesh,  $\delta = 0$  in Figure 6, and the standard Galerkin method,  $p = 1$ . In this example  $k = 20$ .

The similarities with the one dimensional result does not come as a surprise. Since the dual solution is independent of  $y$  in this particular example we can use equation (4.11) to proceed with the following heuristic calculation,

$$-\tau(LU, L\pi\phi)_{\tilde{\Omega}} = (R_\Omega, \phi - \pi\phi) + (R_\Gamma, \phi - \pi\phi)_\Gamma \quad (5.1)$$

$$= \int_0^1 \int_0^1 R_\Omega(\phi - \pi\phi) dy dx \quad (5.2)$$

$$+ \int_{\{x \in [0,1], y=0\}} R_\Gamma(\phi - \pi\phi) dx$$

$$- \int_{\{x \in [0,1], y=1\}} R_\Gamma(\phi - \pi\phi) dx$$

$$\approx \int_0^1 (\phi - \pi\phi) \int_0^1 R_\Omega dy dx + \int_0^1 C(x)(\phi - \pi\phi) dx \quad (5.3)$$

$$= \int_0^1 D(x)(\phi - \pi\phi) dx. \quad (5.4)$$

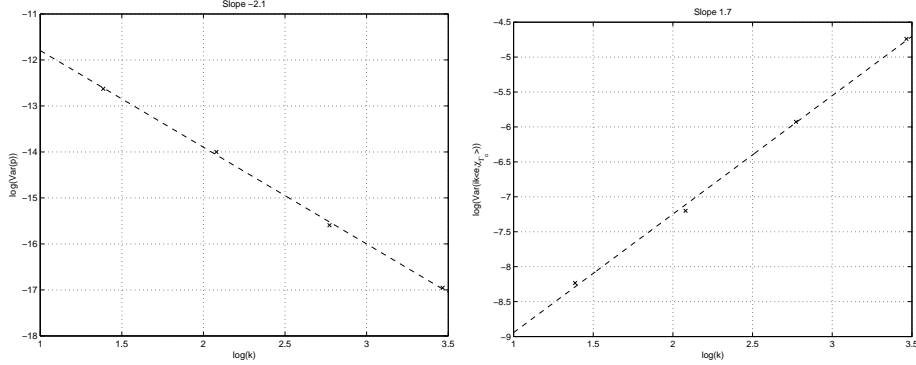


Figure 8:  $\text{Var}(p)$  (left) and  $\text{Var}(ik(e, I_{\Gamma_o})_{\Gamma})$  (right) dependence of  $k$  when  $\delta = 0.3$  and  $kh$  is hold constant.

Using the one dimensional result in equation (2.41) and that  $(LU, L\pi\phi)_{\tilde{\Omega}}$  should not depend heavily on  $\delta$  we get that  $\tau \sim h^2 + C\text{Var}(\delta_x) \sim h^2(1 + C\delta_x^2)$ . The additional assumption we need to do in this case is that also  $\pi\phi$  is almost constant in the  $y$  direction.

We note one difference that actually suggests better results in the two dimensional case when the error is integrated over the outflow boundary. Instead of having essentially  $e = \int R\phi dx$ , where  $R$  is the residual, we get in two dimensions  $e = \int(\int R dy)\phi dx$  i.e. an integral over the residual in the  $y$ -direction. This would decrease the variance of the error and therefore also the error bound by the Chebyshev inequality in equation (2.54).

Numerical results confirms this. We let  $\delta$  and  $hk$  be constant and  $k$  to be free. The variance of  $ik(e, I_{\Gamma_o})_{\Gamma}$  is computed for 100 different meshes in Figure 8. As seen to the left in Figure 8  $\text{Var}(p) \sim (hk)^{\alpha}k^{-2}$  for some  $\alpha$ . With a similar calculation as in the one dimensional case we get  $\text{Var}(ik(e, I_{\Gamma_o})_{\Gamma}) = k^4(U, \pi\phi)^2\text{Var}(p)$  and since  $(U, \pi\phi) \sim 1$  we get  $\text{Var}((e, I_{\Gamma_o})_{\Gamma}) \sim k^2\text{Var}(p) \sim (hk)^{\alpha}$ . We see this in the right plot in Figure 8 where we plot  $\text{Var}(ik(e, I_{\Gamma_o})_{\Gamma})$  verses  $k$  while holding  $hk$  constant. To determine  $\alpha$  we perform another test where we vary  $h$  while holding  $k$  constant. The result is presented in Figure 9. We see that  $\alpha$  is approximately equal to 10 i.e. as we suspected we gain one  $h$  compared to the one dimensional case,

$$\text{Var}((e, I_{\Gamma_o})_{\Gamma}) \sim (hk)^{10}, \quad (5.5)$$

and from the Chebyshev inequality we get from these numerical tests

$$\boxed{P(|(e, I_{\Gamma_o})_{\Gamma}| \leq C(hk)^5) \geq 1 - \epsilon} \quad (5.6)$$

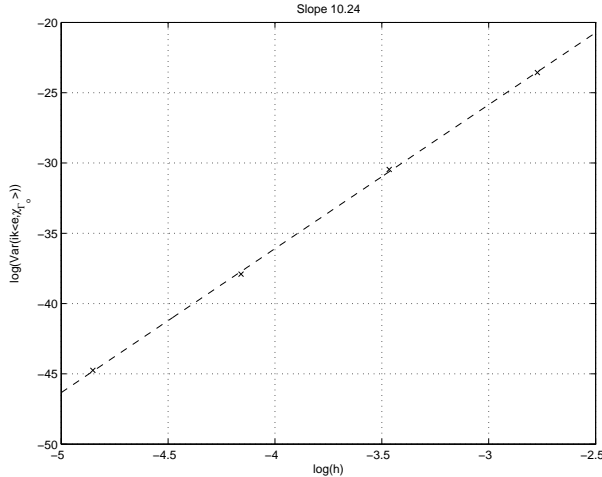


Figure 9:  $\text{Var}(ik(e, I_{\Gamma_o})_{\Gamma})$  versus  $h$  with constant  $k = 4$  and  $\delta = 0.3$ .

for  $\epsilon > 0$  i.e. we have no pollution effect for error control in this specific norm on meshes with constant  $\delta$ .

The variance of the error can also measure the angle depends in the method. With this result we would not expect worse angle dependence when  $k$  increases and  $hk$  is hold constant which is a very nice result.

**Example 2.** Finally we consider a bit more complicated problem where we simulate waves travelling through a slit of width  $\epsilon_y$  and thickness  $\epsilon_x$ . The domain is a rectangle of length  $\pi/2$  and height  $\pi/4$  with two  $\epsilon_x$  wide walls in the middle only leaving a gap of  $\epsilon_y$  between them. The wave number is set to 20 so we expect five full waves in the centre of the domain  $y = \pi/8$ . The real part of the solution of the primal and dual are presented in Figure 10 and Figure 11. The dual solution is calculated for nodal error control in  $(x, y) = (\pi/2, \pi/8)$ . The wave plane propagates towards the slit and creates approximately a point source at the slit. We get the characteristic circular waves as when rocks falls into the sea continuously in one point. The amplitude decreases as the wave propagates away from the slit in the same way as the dual solution decays from the point mass in  $(x, y) = (\pi/2, \pi/8)$ .

## 6 Conclusion

We have discussed how and when standard methods for solving the pollution problem on structured grids needs to be modified to suit unstructured grids.

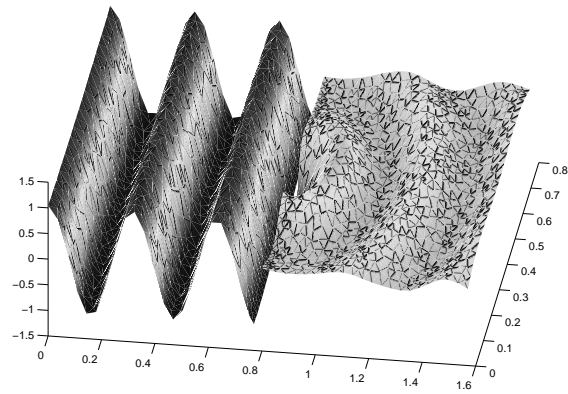


Figure 10: Real part of the solution using our method to determine  $\tau$ .  $\epsilon_x = 0.03$  and  $\epsilon_y = 0.1$ .

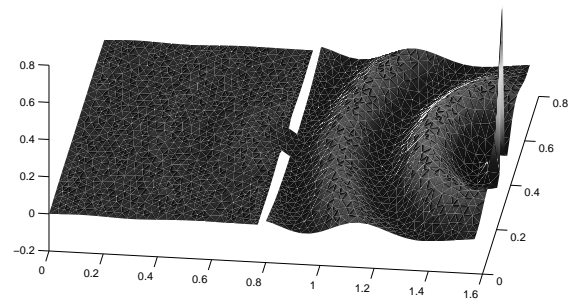


Figure 11: Real part of the dual solution for error control in  $(x, y) = (\pi/2, \pi/8)$ .

The analysis is based on a posteriori error estimates of model problems in one and two dimensions. We present numerical simulations that confirms our theoretical results on both one and two dimensions.

## References

- [1] R. A. Adams, *Sobolev spaces*, volume 65 of Pure and Applied Mathematics, Academic Press, New York, 1975.
- [2] I. Babuška, F. Ihlenburg, E. T. Paik and S. A. Sauter, *A generalised finite element method for solving the Helmholtz equation in two dimensions with minimal pollution*, Comput. Methods Appl. Mech. Engrg., 128(1995), 325-359.
- [3] S. C. Brenner and L. R. Scott, *The mathematical theory of finite element methods*, Springer Verlag, 1994.
- [4] K. Eriksson, D. Estep, P. Hansbo and C. Johnson, *Computational differential equations*, Studentlitteratur, 1996.
- [5] I. Harari and C. L. Nogueira, *Reducing dispersion of linear triangular elements for the Helmholtz equation*, J. of Eng. Mech., 128(3), 351-358, 2002.
- [6] I. Harari and T. J.R. Hughes, *Galerkin/least-squares finite element methods for the reduced wave equation with non-reflecting boundary conditions in unbounded domains*, Comput. Methods Appl. Mech. and Engrg., 98(1992), 411-454.
- [7] T. J.R. Hughes, G. R. Feijóo, L. Mazzei, J.-B. Quincy, *The variational multiscale method - a paradigm for computational mechanics*, Comput. Methods Appl. Mech. and Engrg., 166(1998), 3-24.
- [8] A. A. Oberai and P. M. Pinsky, *A multiscale finite element method for the Helmholtz equation*, Comput. Methods Appl. Mech. Engrg. 154, 281-297, 1998.
- [9] A. A. Oberai and P. M. Pinsky, *A residual-based finite element method for the Helmholtz equation*, Int. J. Numer. Meth. Engng. 49(2000):399-419.
- [10] J.-Y. Wu and R. Lee, *The advantages of triangular and tetrahedral edge elements for electro magnetic modelling with the finite-element method*, IEEE trans. Antennas Propagat., 45(9), 1997.

# Adaptive Variational Multiscale Methods Based on A Posteriori Error Estimation

Mats G. Larson\* and Axel Målqvist†

April 7, 2004

## Abstract

The variational multiscale method (VMM) provides a general framework for construction of multiscale finite element methods. In this paper we propose a method for parallel solution of the fine scale problem based on localized Dirichlet problems which are solved numerically. Next we present a posteriori error estimates for VMM which relates the error in linear functionals and the energy norm to the discretization errors, resolution and size of patches in the localized problems, in the fine scale approximation. Based on the a posteriori error estimates we propose an adaptive VMM with automatic tuning of the critical parameters. We primary study elliptic second order partial differential equations with highly oscillating coefficients or localized singularities.

## 1 Introduction

Many problems in science and engineering involve models of physical systems on many scales. For instance, models of materials with microstructure such as composites and flow in porous media. In such problems it is in general not feasible to seek for a numerical solution which resolves all scales. Instead we may seek to develop algorithms based on a suitable combination a global problem capturing the main features of the solution and localized problems which resolves the fine scales. Since the fine scale problems are localized the computation on the fine scales is parallel in nature.

---

\*Corresponding author, Associate Professor, Department of Mathematics, Chalmers University of Technology, Göteborg, [mgl@math.chalmers.se](mailto:mgl@math.chalmers.se).

†Graduate Research Assistant, Department of Mathematics, Chalmers University of Technology, Göteborg, [axel@math.chalmers.se](mailto:axel@math.chalmers.se).

**Previous work.** The Variational Multiscale Method (VMM) is a general framework for derivation of basic multiscale method in a variational context, see Hughes [8] and [10]. The basic idea is to decompose the solution into fine and coarse scale contributions, solve the fine scale equation in terms of the residual of the coarse scale solution, and finally eliminate the fine scale solution from the coarse scale equation. This procedure leads to a modified coarse scale equation where the modification accounts for the effect of fine scale behavior on the coarse scales. In practice it is necessary to approximate the fine scale equation to make the method realistic. In several works various ways of analytical modeling are investigated often based on bubbles or element Green's functions, see Oberai and Pinsky, [11] and Arbogast [1]. In [7] Hou and Wu present a different approach. Here the fine scale equations are solved numerically on a finer mesh. The fine scale equations are solved inside coarse elements and are thus totally decoupled.

**New contributions.** In this work we present a simple technique for numerical approximation of the fine scale equation in the variational multiscale method. The basic idea is to split the fine scale residual into localized contributions using a partition of unity and solving corresponding decoupled localized problems on patches with homogeneous Dirichlet boundary conditions. The fine scale solution is approximated by the sum  $U_f = \sum_i U_{f,i}$  of the solutions  $U_{f,i}$  to the localized problems. The accuracy of  $U_f$  depends on the fine scale mesh size  $h$  and the size of the patches. We note that the fine scale computation is naturally parallel.

To optimize performance we seek to construct an adaptive algorithm for automatic control of the coarse mesh size  $H$ , the fine mesh size  $h$ , and the size of patches. Our algorithm is based on the following a posteriori estimate of the error  $e = u - U_c - U_f$  in the energy norm for the Poisson equation with variable coefficients  $a$ :

$$\begin{aligned} \|e\|_a \leq C \sum_{i \in \mathcal{C}} \|H\mathcal{R}(U_c)\|_{\omega_i} \left\| \frac{1}{\sqrt{a}} \right\|_{L^\infty(\omega_i)} \\ + C \sum_{i \in \mathcal{F}} \left( \|\sqrt{H}\Sigma(U_{f,i})\|_{\partial\omega_i} + \|h\mathcal{R}_i(U_{f,i})\|_{\omega_i} \right) \left\| \frac{1}{\sqrt{a}} \right\|_{L^\infty(\omega_i)}, \end{aligned} \quad (1.1)$$

where

$$(-\Sigma(U_{f,i}), v_f)_{\partial\omega_i} = (f + \nabla \cdot a \nabla U_c, \varphi_i v_f)_{\omega_i} - a(U_{f,i}, v_f)_{\omega_i}, \quad \text{for all } v_f \in V_f^h(\bar{\omega}_i), \quad (1.2)$$

$\mathcal{C}$  refers to nodes where no local problems have been solved,  $\mathcal{F}$  to nodes where local problems are solved,  $U_c$  is the coarse scale solution,  $U = U_c + U_f$ ,  $\mathcal{R}(U)$  is a computable bound of the residual  $f + \nabla \cdot a \nabla U$ ,  $\mathcal{R}_i(U_{f,i})$  is a bound of

the fine scale residual  $\varphi_i(f + \nabla \cdot a \nabla U_c) + \nabla \cdot a \nabla U_{f,i}$ ,  $\Sigma(U_{f,i})$  is related to the normal derivative of the fine scale solution  $U_{f,i}$  and measures the effect of restriction to patches. If no fine scale equations are solved we obtain the first term in the estimate; the first part of the second sum measures the effect of restriction to patches; and finally the second part measures the influence of the fine scale mesh parameter  $h$ .

In addition to the energy norm error estimate we also derive error representation formulas for errors in linear functionals of the computed solution using duality techniques. The framework is fairly general and may be extended to other types of multiscale methods, for instance, based on localized Neumann problems.

**Outline.** In Section 2 we introduce the model problem and the variational multiscale formulation of this problem we also discuss the split of the coarse and fine scale spaces. In Section 3 we present a posteriori estimates of the error leading to Section 4 where we present an adaptive algorithm. In section Section 5 we present numerical results and finally Section 6 consists of concluding remarks and suggestions on future work.

## 2 The Variational Multiscale Method

### 2.1 Model Problem

We study the Poisson equation with a highly oscillating coefficient  $a$  and homogeneous Dirichlet boundary conditions: find  $u \in H_0^1(\Omega)$  such that

$$-\nabla \cdot a \nabla u = f \quad \text{in } \Omega, \quad (2.1)$$

where  $\Omega$  is a polygonal domain in  $\mathbf{R}^d$ ,  $d = 1, 2$ , or  $3$  with boundary  $\Gamma$ ,  $f \in H^{-1}(\Omega)$ , and  $a \in L^\infty(\Omega)$  such that  $a(x) \geq \alpha_0 > 0$  for all  $x \in \Omega$ . The variational form of (2.1) reads: find  $u \in \mathcal{V} = H_0^1(\Omega)$  such that

$$a(u, v) = (f, v) \quad \text{for all } v \in \mathcal{V}, \quad (2.2)$$

with the bilinear form

$$a(u, v) = (a \nabla u, \nabla v) \quad (2.3)$$

for all  $u, v \in \mathcal{V}$ .

### 2.2 The Variational Multiscale Method

We employ the variational multiscale scale formulation, proposed by Hughes see [8, 10] for an overview, and introduce a coarse and a fine scale in the

problem. We choose two spaces  $\mathcal{V}_c \subset \mathcal{V}$  and  $\mathcal{V}_f \subset \mathcal{V}$  such that

$$\mathcal{V} = \mathcal{V}_c \oplus \mathcal{V}_f. \quad (2.4)$$

Then we may pose (2.2) in the following way: find  $u_c \in \mathcal{V}_c$  and  $u_f \in \mathcal{V}_f$  such that

$$\begin{aligned} a(u_c, v_c) + a(u_f, v_c) &= (f, v_c) \quad \text{for all } v_c \in \mathcal{V}_c, \\ a(u_c, v_f) + a(u_f, v_f) &= (f, v_f) \quad \text{for all } v_f \in \mathcal{V}_f. \end{aligned} \quad (2.5)$$

Introducing the residual  $R : \mathcal{V} \rightarrow \mathcal{V}'$  defined by

$$(R(v), w) = (f, w) - a(v, w) \quad \text{for all } w \in \mathcal{V}, \quad (2.6)$$

the fine scale equation takes the form: find  $u_f \in \mathcal{V}_f$  such that

$$(f, v_f) - a(u_f, v_f) = (R(u_c), v_f) \quad \text{for all } v_f \in \mathcal{V}_f. \quad (2.7)$$

Thus the fine scale solution is driven by the residual of the coarse scale solution. Denoting the solution  $u_f$  to (2.7) by  $u_f = TR(u_c)$  we get the modified coarse scale problem

$$a(u_c, v_c) + a(TR(u_c), v_c) = (f, v_c) \quad \text{for all } v_c \in \mathcal{V}_c. \quad (2.8)$$

Here the second term on the left hand side accounts for the effects of fine scales on the coarse scales.

### 2.3 A VMM Based on Localized Dirichlet Problems

We introduce a partition  $\mathcal{K} = \{K\}$  of the domain  $\Omega$  into shape regular elements  $K$  of diameter  $H_K$  and we let  $\mathcal{N}$  be the set of nodes. Further we let  $\mathcal{V}_c$  be the space of continuous piecewise polynomials of degree  $p$  defined on  $\mathcal{K}$ .

We shall now construct an algorithm which approximates the fine scale equation by a set of decoupled localized problems. We begin by writing  $u_f = \sum_{i \in \mathcal{N}} u_{f,i}$  where

$$a(u_{f,i}, v_f) = (\varphi_i R(u_c), v_f) \quad \text{for all } v_f \in \mathcal{V}_f, \quad (2.9)$$

and  $\{\varphi_i\}_{i \in \mathcal{N}}$  is the set of Lagrange basis functions in  $\mathcal{V}_c$ . Note that  $\{\varphi_i\}_{i \in \mathcal{N}}$  is a partition of unity with support on the elements sharing the node  $i$ . We call the set of elements with one corner in node  $i$  a mesh star in node  $i$  and denote it  $S_1^i$ . Thus functions  $u_{f,i}$  correspond to the fine scale effects created by the localized residuals  $\varphi_i R(u_c)$ . Introducing this expansion of  $u_f$  in the right hand side of the fine scale equation (2.5) and get: find  $u_c \in \mathcal{V}_c$  and  $u_f = \sum_{i \in \mathcal{N}} u_{f,i} \in \mathcal{V}_f$  such that

$$\begin{aligned} a(u_c, v_c) + a(u_f, v_c) &= (f, v_c) \quad \text{for all } v_c \in \mathcal{V}_c, \\ a(u_{f,i}, v_f) &= (\varphi_i R(u_c), v_f) \quad \text{for all } v_f \in \mathcal{V}_f \text{ and } i \in \mathcal{N}. \end{aligned} \quad (2.10)$$

We use this fact to construct a finite element method for solving (2.10) approximately in two steps.

- For each coarse node we define a patch  $\omega_i$  such that  $\text{supp}(\varphi_i) \subset \omega_i \subset \Omega$ . We denote the boundary of  $\omega_i$  by  $\partial\omega_i$ .
- On these patches we define piecewise polynomial spaces  $\mathcal{V}_f^h(\omega_i)$  with respect to a fine mesh with mesh function  $h = h(x)$  defined as a piecewise constant function on the fine mesh. Functions in  $\mathcal{V}_f^h(\omega_i)$  are equal to zero on  $\partial\omega_i$ .

The resulting method reads: find  $U_c \in \mathcal{V}_c$  and  $U_f = \sum_i^n U_{f,i}$  where  $U_{f,i} \in \mathcal{V}_f^h(\omega_i)$  such that

$$\begin{aligned} a(U_c, v_c) + a(U_f, v_c) &= (f, v_c) \quad \text{for all } v_c \in \mathcal{V}_c, \\ a(U_{f,i}, v_f) &= (\varphi_i R(U_c), v_f) \quad \text{for all } v_f \in \mathcal{V}_f^h(\omega_i) \text{ and } i \in \mathcal{N}. \end{aligned} \quad (2.11)$$

Since the functions in the local finite element spaces  $\mathcal{V}_f^h(\omega_i)$  are equal to zero on  $\partial\omega_i$ ,  $U_f$  and therefore  $U$  will be continuous.

**Remark 2.1** For problems with multiscale phenomena on a part of the domain it is not necessary to solve local problems for all coarse nodes. We let  $\mathcal{C} \subset \mathcal{N}$  refer to nodes where no local problems are solved and  $\mathcal{F} \subset \mathcal{N}$  refer to nodes where local problems are solved. Obviously  $\mathcal{C} \cup \mathcal{F} = \mathcal{N}$ . We let  $U_{f,i} = 0$  for  $i \in \mathcal{C}$ .

**Remark 2.2** The choice of the subdomains  $\omega_i$  is crucial for the method. We introduce a notation for extended stars of many layers of coarse elements recursively in the following way. The extended mesh star  $S_L^i = \cup_{j \in S_{L-1}^i} S_1^j$  for  $L > 1$ . We refer to  $L$  as layers, see Figure 1.

## 2.4 Subspaces

The choice of the fine scale space  $\mathcal{V}_f$  can be done in different ways. In a paper by Aksoylu and Holst [4] three suggestions are made.

**Hierarchical basis method.** The first and perhaps easiest approach is to let  $\mathcal{V}_f = \{v \in \mathcal{V} : v(x_j) = 0, j = \mathcal{N}\}$ , where  $\{x_i\}_{i \in \mathcal{N}}$  are the coarse mesh nodes. When  $\mathcal{V}_f$  is discretized by the standard piecewise polynomials on the fine mesh this means that the fine scale base functions will have support on fine scale stars.

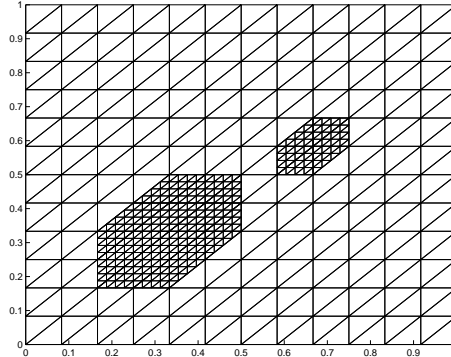


Figure 1: Two (left) and one (right) layer stars.

**BPX preconditioner.** The second approach is to let  $\mathcal{V}_f$  be  $L^2(\Omega)$  orthogonal to  $\mathcal{V}_c$ . In this case we will have global support for the fine scale base functions but for the discretized space we have rapid decay outside fine mesh stars.

**Wavelet modified hierarchical basis method.** The third choice is a mix of the other two. The fine scale space  $\mathcal{V}_f$  is defined as an approximate  $L^2(\Omega)$  orthogonal version of the Hierarchical basis method. We let  $Q_c^a v \in \mathcal{V}_c$  be an approximate solution (a small number of Jacobi iterations) to

$$(Q_c^a v, w) = (v, w), \quad \text{for all } w \in \mathcal{V}_c. \quad (2.12)$$

and define the Wavelet modified hierarchical basis function associated with the hierarchical basis function  $\varphi_{HB}$  to be,

$$\varphi_{WHB} = (I - Q_c^a)\varphi_{HB}, \quad (2.13)$$

see Figure 2.

For an extended description of these methods see [3, 4, 2]. In this paper we focus on the WHB method.

## 3 A Posteriori Error Estimates

### 3.1 The Dual Problem

To derive a posteriori error estimates of the error in a given linear functional  $(e, \psi)$  with  $e = u - U$  and  $\psi \in H^{-1}(\Omega)$  a given weight. We introduce the following dual problem: find  $\phi \in \mathcal{V}$  such that

$$a(v, \phi) = (v, \psi) \quad \text{for all } v \in \mathcal{V}. \quad (3.1)$$

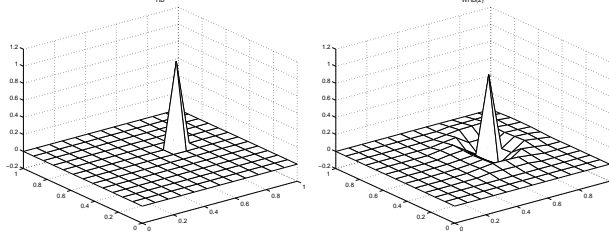


Figure 2: HB-function and WHB-function with two Jacobi iterations.

In the VMM setting this yields: find  $\phi_c \in \mathcal{V}_c$  and  $\phi_f \in \mathcal{V}_f$  such that

$$\begin{aligned} a(v_c, \phi_c) + a(v_c, \phi_f) &= (v_c, \psi), \quad \text{for all } v_c \in \mathcal{V}_c, \\ a(v_f, \phi_f) + a(v_f, \phi_c) &= (v_f, \psi), \quad \text{for all } v_f \in \mathcal{V}_f. \end{aligned} \quad (3.2)$$

### 3.2 Error Representation Formula

We now derive an error representation formula involving both the coarse scale error  $e_c = u_c - U_c$  and the fine scale error  $e_f = \sum_{i \in \mathcal{N}} e_{f,i} := \sum_{i \in \mathcal{N}} (u_{f,i} - U_{f,i})$  that arises from using our finite element method (2.11).

We use the dual problem (3.2) to derive an a posteriori error estimate for a linear functional of the error  $e = e_c + e_f$ . If we subtract the coarse part of equation (2.11) from the coarse part of equation (2.10) we get the Galerkin orthogonality,

$$a(e_c, v_c) + a(e_f, v_c) = 0 \quad \text{for all } v_c \in \mathcal{V}_c. \quad (3.3)$$

The same argument on the fine scale equation gives for  $i \in \mathcal{F}$ ,

$$a(e_{f,i}, v_f) = (f, \varphi_i v_f) - a(e_c, \varphi_i v_f), \quad \text{for all } v_f \in \mathcal{V}_f^h(\omega_i). \quad (3.4)$$

We are now ready to state the an error representation formula.

**Theorem 3.1** *If  $\psi \in H^{-1}(\Omega)$  then,*

$$(e, \psi) = \sum_{i \in \mathcal{C}} (\varphi_i R(U), \phi_f) + \sum_{i \in \mathcal{F}} \left( (\varphi_i R(U_c), \phi_f - v_{f,i}^h)_{\omega_i} - a(U_{f,i}, \phi_f^h - v_{f,i}^h)_{\omega_i} \right) \quad (3.5)$$

for all  $v_{f,i}^h \in \mathcal{V}_f^h(\omega_i)$  and  $i \in \mathcal{F}$ .

**Proof.** Starting from the definition of the dual problem and letting  $v = e =$

$u - U_c - U_f$  we get

$$(e, \psi) = a(e, \phi) \quad (3.6)$$

$$= a(e, \phi_f) \quad (3.7)$$

$$= a(u - U_c, \phi_f) - a(U_f, \phi_f) \quad (3.8)$$

$$= (R(U_c), \phi_f) - a(U_f, \phi_f) \quad (3.9)$$

$$= (R(U_c), \phi_f) - \sum_{i \in \mathcal{F}} a(U_{f,i}, \phi_f) \quad (3.10)$$

$$= \sum_{i \in \mathcal{C}} (\varphi_i R(U_c), \phi_f) \quad (3.11)$$

$$+ \sum_{i \in \mathcal{F}} (\varphi_i R(U_c), \phi_f) - a(U_{f,i}, \phi_f). \quad (3.12)$$

Since equation (2.11) holds we can subtract functions  $v_{f,i}^h \in \mathcal{V}_f^h(\omega_i)$  where  $i \in \mathcal{F}$  from equation (3.12). We end up with

$$(e, \psi) = \sum_{i \in \mathcal{C}} (\varphi_i R(U_c), \phi_f) + \sum_{i \in \mathcal{F}} (\varphi_i R(U_c), \phi_f - v_{f,i}^h) - a(U_{f,i}, \phi_f - v_{f,i}^h), \quad (3.13)$$

which proves the theorem.  $\square$

For example we can choose  $v_f^h = \pi_h \phi_f$ , where  $\pi_h \phi_f$  is the Scott-Zhang interpolant of  $\phi_f$  onto  $\mathcal{V}_f^h(\omega_i)$ .

**Remark 3.1** In practice the dual problem has to be solved numerically and the solution has to be in a finer space than the primal solution. To achieve this we can increase the number of layers when solving the dual problem.

### 3.3 Energy Norm Estimate

Next we introduce a notation for a bound of the residual. Let  $\mathcal{R}(U)$  be a bound of the residual defined in the following way, see [6]:

$$\mathcal{R}(U) = |f + \nabla \cdot a \nabla U| + \frac{1}{2} \max_{K \in \mathcal{K}} h_K^{-1} |[a \partial_n U]| \quad \text{on } K \in \mathcal{K}, \quad (3.14)$$

where  $\mathcal{K}$  is the set of elements in the mesh and  $[\cdot]$  is the difference in function value over the current interior edge. We note that  $|(R(U), v)| \leq \|h^s \mathcal{R}(U)\| \|h^{-s} v\|$  for  $s \in \mathbf{R}$ . We define  $\mathcal{R}_i(U_{f,i})$  in the same way as  $\mathcal{R}(U)$  on the local mesh but with  $U$  replaced by  $U_{f,i}$  and  $f$  replaced by  $\varphi_i \mathcal{R}(U_c)$ .

We also define a new space on the patches. Let  $V_f^h(\bar{\omega}_i)$  be the space of piecewise polynomials of degree  $p$  on  $\omega_i$ . This space is identical to  $V_f^h(\omega_i)$

with the difference that  $V_f^h(\bar{\omega}_i)$  is not necessarily zero on the boundary  $\partial\omega_i$ . This means that  $V_f^h(\omega_i) \subset V_f^h(\bar{\omega}_i)$ .

We now state the following estimate for the error in the energy norm,  $\|e\|_a = a(e, e)^{1/2}$ .

**Theorem 3.2** *It holds,*

$$\begin{aligned} \|e\|_a &\leq C \sum_{i \in \mathcal{C}} \|H\mathcal{R}(U_c)\|_{\omega_i} \left\| \frac{1}{\sqrt{a}} \right\|_{L^\infty(\omega_i)} \\ &\quad + C \sum_{i \in \mathcal{F}} \left( \|\sqrt{H}\Sigma(U_{f,i})\|_{\partial\omega_i} + \|h\mathcal{R}_i(U_{f,i})\|_{\omega_i} \right) \left\| \frac{1}{\sqrt{a}} \right\|_{L^\infty(\omega_i)}, \end{aligned} \quad (3.15)$$

where

$$(-\Sigma(U_{f,i}), v_f)_{\partial\omega_i} = (\varphi_i R(U_c), v_f)_{\omega_i} - a(U_{f,i}, v_f)_{\omega_i}, \quad \text{for all } v_f \in V_f^h(\bar{\omega}_i). \quad (3.16)$$

**Proof.** We start with similar arguments as in the proof of Theorem 3.1. We use the error equation (3.3) with  $v_c$  as the Scott-Zhang interpolant  $\pi_c e$  onto the coarse space  $\mathcal{V}_c$ , see [5], to get,

$$\|e\|_a^2 = a(e, e) \quad (3.17)$$

$$= a(e, e - \pi_c e) \quad (3.18)$$

$$= a(u - U_c, e - \pi_c e) - a(U_f, e - \pi_c e) \quad (3.19)$$

$$= (R(U_c), e - \pi_c e) - a(U_f, e - \pi_c e) \quad (3.20)$$

$$= \sum_{i \in \mathcal{C}} (\varphi_i R(U_c), e - \pi_c e) \quad (3.21)$$

$$\begin{aligned} &\quad + \sum_{i \in \mathcal{F}} (\varphi_i R(U_c), e - \pi_c e) - a(U_{f,i}, e - \pi_c e) \\ &= \sum_{i \in \mathcal{C}} (\varphi_i R(U_c), e - \pi_c e) \end{aligned} \quad (3.22)$$

$$\begin{aligned} &\quad + \sum_{i \in \mathcal{F}} (\varphi_i R(U_c), \pi_{f,i}(e - \pi_c e)) - a(U_{f,i}, \pi_{f,i}(e - \pi_c e)) \\ &\quad + \sum_{i \in \mathcal{F}} (\varphi_i R(U_c), e - \pi_c e - \pi_{f,i}(e - \pi_c e)) \\ &\quad - \sum_{i \in \mathcal{F}} a(U_{f,i}, e - \pi_c e - \pi_{f,i}(e - \pi_c e)) \\ &= \text{I} + \text{II} + \text{III} \end{aligned} \quad (3.23)$$

where  $\pi_{f,i}$  is the Scott-Zhang interpolant onto  $\mathcal{V}_f(\omega_i)$ . We start by estimating the first term of equation (3.23), I. From interpolation theory [5] we have,

$$\sum_{i \in \mathcal{C}} (\varphi_i R(U_c), e - \pi_c e) \leq \sum_{i \in \mathcal{C}} \|\varphi_i R(U_c)\|_{\omega_i} \|e - \pi_c e\|_{\omega_i} \quad (3.24)$$

$$\leq C \sum_{i \in \mathcal{C}} \|H \mathcal{R}(U_c)\|_{\omega_i} \|\nabla e\|_{\omega_i}. \quad (3.25)$$

Next we turn our attention to the second term of equation (3.23), II. We introduce  $\Sigma(U_{f,i})$  which is the piecewise polynomial defined on  $\partial\omega_i$  that uniquely solves,

$$(-\Sigma(U_{f,i}), v_f)_{\partial\omega_i} = (R(U_c), \varphi_i v_f)_{\omega_i} - a(U_{f,i}, v_f)_{\omega_i}, \quad \text{for all } v_f \in V_f^h(\bar{\omega}_i). \quad (3.26)$$

With this definition we get the following estimate for the second term,

$$\text{II} = \sum_{i \in \mathcal{F}} (-\Sigma(U_{f,i}), \pi_{f,i}(e - \pi_c e))_{\partial\omega_i} \quad (3.27)$$

$$\leq \sum_{i \in \mathcal{F}} \|\sqrt{H} \Sigma(U_{f,i})\|_{\partial\omega_i} \left\| \frac{1}{\sqrt{H}} \pi_{f,i}(e - \pi_c e) \right\|_{\partial\omega_i}. \quad (3.28)$$

We use the following trace inequality from [5],

$$\|\pi_{f,i}(e - \pi_c e)\|_{\partial\omega_i}^2 \leq C \left( \frac{1}{H} \|\pi_{f,i}(e - \pi_c e)\|_{\omega_i}^2 + H \|\nabla \pi_{f,i}(e - \pi_c e)\|_{\omega_i}^2 \right). \quad (3.29)$$

Next we use that the Scott-Zhang interpolant is both  $L^2$  and  $H^1$  stable from [5] to get,

$$\|\pi_{f,i}(e - \pi_c e)\|_{\partial\omega_i}^2 \leq C \left( \frac{1}{H} \|e - \pi_c e\|_{\omega_i}^2 + H \|\nabla(e - \pi_c e)\|_{\omega_i}^2 \right) \quad (3.30)$$

$$\leq CH \|\nabla e\|_{\omega_i}^2. \quad (3.31)$$

We conclude

$$\text{II} \leq C \sum_{i \in \mathcal{F}} \|\sqrt{H} \Sigma(U_{f,i})\|_{\partial\omega_i} \|\nabla e\|_{\omega_i}. \quad (3.32)$$

We now take on the third term in equation (3.23),  $\sum_{i \in \mathcal{F}} (\varphi_i R(U_c), e - \pi_c e - \pi_{f,i}(e - \pi_c e)) - a(U_{f,i}, e - \pi_c e - \pi_{f,i}(e - \pi_c e))$ ,

$$\text{III} \leq C \sum_{i \in \mathcal{F}} \|h \mathcal{R}_i(U_{f,i})\|_{\omega_i} \|\nabla(e - \pi_c e)\|_{\omega_i} \quad (3.33)$$

$$\leq C \sum_{i \in \mathcal{F}} \|h \mathcal{R}_i(U_{f,i})\|_{\omega_i} \|\nabla e\|_{\omega_i}. \quad (3.34)$$

We need to do the following simple observation,

$$\|\nabla e\|_{\omega_i} \leq \left\| \frac{1}{\sqrt{a}} \right\|_{L^\infty(\omega_i)} \|\sqrt{a} \nabla e\|_{\omega_i}, \quad (3.35)$$

by Hölder's inequality. We go back to equation (3.17) and use the estimates of the three terms together with equation (3.35)

$$\|e\|_a^2 \leq \sum_{i \in \mathcal{C}} (\varphi_i R(U_c), e - \pi_c e) \quad (3.36)$$

$$\begin{aligned} &+ \sum_{i \in \mathcal{F}} (\varphi_i R(U_c), \pi_{f,i}(e - \pi_c e)) - a(U_{f,i}, \pi_{f,i}(e - \pi_c e)) \\ &+ \sum_{i \in \mathcal{F}} (\varphi_i R(U_c), e - \pi_c e - \pi_{f,i}(e - \pi_c e)) \\ &- \sum_{i \in \mathcal{F}} a(U_{f,i}, e - \pi_c e - \pi_{f,i}(e - \pi_c e)) \\ &\leq C \sum_{i \in \mathcal{C}} \|H\mathcal{R}(U_c)\|_{\omega_i} \|\nabla e\|_{\omega_i} \quad (3.37) \end{aligned}$$

$$\begin{aligned} &+ C \sum_{i \in \mathcal{F}} \|\sqrt{H}\Sigma(U_{f,i})\|_{\partial\omega_i} \|\nabla e\|_{\omega_i} \\ &+ C \sum_{i \in \mathcal{F}} \|h\mathcal{R}_i(U_{f,i})\|_{\omega_i} \|\nabla e\|_{\omega_i} \\ &\leq C \left( \sum_{i \in \mathcal{C}} \|H\mathcal{R}(U_c)\|_{\omega_i} \left\| \frac{1}{\sqrt{a}} \right\|_{L^\infty(\omega_i)} \right) \|e\|_a \quad (3.38) \\ &+ C \left( \sum_{i \in \mathcal{F}} \|\sqrt{H}\Sigma(U_{f,i})\|_{\partial\omega_i} \left\| \frac{1}{\sqrt{a}} \right\|_{L^\infty(\omega_i)} \right) \|e\|_a \\ &+ C \left( \sum_{i \in \mathcal{F}} \|h\mathcal{R}_i(U_{f,i})\|_{\omega_i} \left\| \frac{1}{\sqrt{a}} \right\|_{L^\infty(\omega_i)} \right) \|e\|_a \end{aligned}$$

Finally we get

$$\begin{aligned} \|e\|_a &\leq C \sum_{i \in \mathcal{C}} \|H\mathcal{R}(U_c)\|_{\omega_i} \left\| \frac{1}{\sqrt{a}} \right\|_{L^\infty(\omega_i)} \quad (3.39) \\ &+ C \sum_{i \in \mathcal{F}} \left( \|\sqrt{H}\Sigma(U_{f,i})\|_{\partial\omega_i} + \|h\mathcal{R}_i(U_{f,i})\|_{\omega_i} \right) \left\| \frac{1}{\sqrt{a}} \right\|_{L^\infty(\omega_i)}, \end{aligned}$$

which proves the theorem.  $\square$

**Remark 3.2** We need to motivate the definition of  $\Sigma(U_{f,i})$ :

$$(-\Sigma(U_{f,i}), v_f)_{\partial\omega_i} = (\varphi_i R(U_c), v_f)_{\omega_i} - (a\nabla U_{f,i}, \nabla v_f)_{\omega_i}, \quad \text{for all } v_f \in V_f^h(\bar{\omega}_i), \quad (3.40)$$

in equation (3.16). The function  $\Sigma(U_{f,i})$  is a piecewise polynomial defined on the boundary of patch  $\omega_i$ . Remember that

$$(\varphi_i R(U_c), v_f)_{\omega_i} - (a\nabla U_{f,i}, \nabla v_f)_{\omega_i} = 0, \quad \text{for all } v_f \in V_f^h(\bar{\omega}_i), \quad (3.41)$$

This means that have the same number of unknowns and equations and in practice calculating  $\Sigma(U_{f,i})$  will come down to solving a linear system with a mass matrix defined on the boundary of the patch. There is a close connection between  $\Sigma(U_{f,i})$  and  $n \cdot a\nabla U_{f,i}$  in fact  $\Sigma(U_{f,i})$  is the  $L^2(\partial\omega_i)$  projection of  $n \cdot a\nabla U_{f,i}$ . This is further discussed in [9].

### 3.4 Application to A Posteriori Error Estimates for the Standard Galerkin Method

We use the variational multiscale method on a dual problem to estimate the error of the standard Galerkin solution on the coarse mesh: find  $U \in \mathcal{V}_c$  such that

$$a(U, v) = (f, v), \quad \text{for all } v \in \mathcal{V}_c. \quad (3.42)$$

The corresponding discrete variational multiscale method for the dual reads: find  $\Phi_c \in \mathcal{V}_c$  and  $\Phi_f = \sum_{i \in \mathcal{N}} \Phi_{f,i}$  where  $\Phi_{f,i} \in \mathcal{V}_f^h(\omega_i)$  such that

$$\begin{aligned} a(v_c, \Phi_c) + a(v_c, \Phi_f) &= (v_c, \psi) \quad \text{for all } v_c \in \mathcal{V}_c, \\ a(v_f, \Phi_{f,i}) &= (\varphi_i v_f, \psi) - a(\varphi_i v_f, \Phi_c) \quad \text{for all } v_f \in \mathcal{V}_f^h(\omega_i). \end{aligned} \quad (3.43)$$

Since we have  $a(u, v) = (f, v)$  for all  $v \in \mathcal{V}_c$  we can subtract equation (3.42) from this equation to get the Galerkin orthogonality,

$$a(u - U, v) = 0, \quad \text{for all } v \in \mathcal{V}_c. \quad (3.44)$$

We formulate an error representation formula for the standard Galerkin method in the following proposition.

**Proposition 3.1** *It holds*

$$(u - U, \psi) = \sum_{i \in \mathcal{N}} (R(U), \Phi_{f,i}) + (R(U), \phi_f - \Phi_f). \quad (3.45)$$

**Proof.** Together equation (3.44) and equation (3.2) gives

$$(u - U, \psi) = a(u, \phi_c + \phi_f) - a(U, \phi_c + \phi_f) \quad (3.46)$$

$$= (f, \phi_c + \phi_f) - a(U, \phi_c + \phi_f) \quad (3.47)$$

$$= (R(U), \phi_f) \quad (3.48)$$

Finally we add and subtract the  $\Phi_f$  term.  $\square$

If we can get a bound of  $\phi_f - \Phi_f$  in terms of the fine mesh parameter  $h$  and the size of the subdomains  $\omega_i$ , the computable terms  $(R(U), \Phi_{f,i})$  will serve as local error estimators that points out elements where the fine scale influence is significant. This is done in the following theorem

**Theorem 3.3** *It holds,*

$$\begin{aligned} |(R(U), \phi_f - \Phi_f)| &\leq C_a \|HR(U)\| \sum_{i \in \mathcal{N}} \|\sqrt{H}\Sigma(\Phi_{f,i})\|_{\partial\omega_i} \frac{1}{\sqrt{a}} \|L^\infty(\omega_i)\| \quad (3.49) \\ &+ C_a \|HR(U)\| \sum_{i \in \mathcal{N}} \|h\mathcal{R}_i(\Phi_{f,i})\|_{\omega_i} \frac{1}{\sqrt{a}} \|L^\infty(\omega_i)\|, \end{aligned}$$

where

$$(\Sigma(\Phi_{f,i}), v_f)_{\partial\omega_i} = a(\Phi_{f,i}, v_f)_{\omega_i} - (\psi + \nabla \cdot a \nabla \Phi_c, v_f)_{\omega_i}, \quad \text{for all } v_f \in V_f^h(\bar{\omega}_i), \quad (3.50)$$

and  $\mathcal{R}_i(\Phi_{f,i})$  is defined in analogy with with the earlier definition for  $\mathcal{R}_i(U_{f,i})$ .

**Proof.** We start with the rest term of equation (3.45),

$$|(R(U), \phi_f - \Phi_f)| = |a(e, \phi_f - \Phi_f)| \quad (3.51)$$

$$\leq \|e\|_a \|\phi_f - \Phi_f\|_a \quad (3.52)$$

$$\leq \|e\|_a \|\phi - (\Phi_c + \Phi_f)\|_a. \quad (3.53)$$

From standard a posteriori theory we know that  $\|e\|_a \leq C_a \|HR(U)\|$ , for some constant  $C_a$  depending on  $a$ , and from Theorem 3.2 with  $f = \psi$ ,  $u = \phi$ ,  $U_c = \Phi_c$ ,  $U_f = \Phi_f$ ,  $\mathcal{C} = \emptyset$ , and  $U_{f,i} = \Phi_{f,i}$  we have,

$$\begin{aligned} \|\phi - (\Phi_c + \Phi_f)\|_a &\leq C \sum_{i \in \mathcal{N}} \|\sqrt{H}\Sigma(\Phi_{f,i})\|_{\partial\omega_i} \frac{1}{\sqrt{a}} \|L^\infty(\omega_i)\| \quad (3.54) \\ &+ C \sum_{i \in \mathcal{N}} \|h\mathcal{R}_i(\Phi_{f,i})\|_{\omega_i} \frac{1}{\sqrt{a}} \|L^\infty(\omega_i)\|, \end{aligned}$$

with  $\Sigma(\Phi_{f,i})$  defined as in equation (3.50). The theorem follows immediately by combining equation (3.53) and equation (3.54).  $\square$

## 4 Adaptive Algorithm

We use the energy norm estimate in Theorem 3.2 to construct an adaptive algorithm. We remember the result,

$$\begin{aligned} \|e\|_a \leq C \sum_{i \in \mathcal{C}} \|H\mathcal{R}(U_c)\|_{\omega_i} \frac{1}{\sqrt{a}} \|L^\infty(\omega_i) & \quad (4.1) \\ + C \sum_{i \in \mathcal{F}} \left( \|\sqrt{H}\Sigma(U_{f,i})\|_{\partial\omega_i} + \|h\mathcal{R}_i(U_{f,i})\|_{\omega_i} \right) \frac{1}{\sqrt{a}} \|L^\infty(\omega_i), & \end{aligned}$$

These contributions to the error can easily be understood. The first term is the standard a posteriori estimate for a Galerkin solution on the coarse mesh i.e. this is what we get if we do not solve any local problems. The first part of the second sum represents the error arising from the fact that we solve the local problems on patches  $\omega_i$  instead of the whole domain. Remember that  $\Sigma(U_{f,i})$  is closely related to the normal derivative of the fine scale solution on the boundary of the patches. Finally, the second part of the second sum represents the fine scale resolution. The two contributions to the second sum clearly points out the parameters of interest when using our method. The first one is the patch size, increasing patch size will decrease  $\|\sqrt{H}\Sigma_i\|_{\partial\omega_i}$ , the second one is the fine scale mesh size  $h$ .

From equation (4.1) we now state the following adaptive algorithm:

### Adaptive Algorithm.

- Start with no nodes in  $\mathcal{F}$ .
- Calculate a solution  $U$  on the coarse mesh.
- Calculate the residuals for each coarse node,  $R_i = \|H\mathcal{R}(U_c)\|_{\omega_i}$ .
- Calculate the contributions from the first term of the local problems,  $S_i = \|\sqrt{H}\Sigma_i\|_{\partial\omega_i}$ .
- Calculate the contributions from the second term of the local problems,  $W_i = \|h\mathcal{R}_i(U_{f,i})\|_{\omega_i}$ .
- For large values in  $R_i$  add  $i$  to  $\mathcal{F}$ , for large values in  $S_i$  or  $W_i$  either increase the number of layers or decrease the fine scale mesh size  $h$  for local problem  $i$ . Return to 2 or stop if the desired tolerance is reached.

## 5 Numerical Examples

We solve two dimensional model problems with linear base functions defined on a uniform triangular mesh.

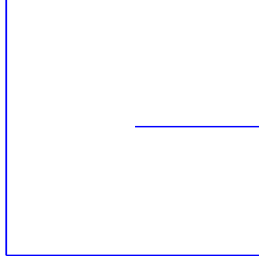


Figure 3: Unit square with a slit between  $(0.5, 0.5)$  and  $(1, 0.5)$ .

**Example 1.** In the first example we let  $a = 1$ ,  $f = 1$ , and  $\Omega$  be the unit square with a slit, see Figure 5. The solution  $u$  is forced to be zero on the boundary including the slit. We solve the problem by using the adaptive algorithm above with a refinement level of 10 % each iteration. Figure 5 shown the adaptive choice of refinement level  $k$ , where  $h = H \cdot 2^{-k}$ , and number of layers  $L$  for the local problems after one and two iterations. We plot the difference between our solution and a reference solution in Figure 5. We see that the Galerkin solution has a large error in the singularity and that we can take care of this singularity by solving local problems chosen in an adaptive fashion.

**Example 2.** In this example we use a simple geometry, the unit square, but we let the coefficient  $a$  oscillate rapidly according to Figure 5. We calculate a reference solution on the fine space and compare it to the standard Galerkin on the coarse mesh with and without solving local problems. We see that standard Galerkin on a coarse mesh performs badly for this problem, Figure 5. Solving local problems using one layer stars give the solution the correct magnitude and if we use two layers we see that the fine scale features of the solution starts to fall into place. In this example no adaptivity was used. Local problems was solved for all coarse nodes.

## 6 Conclusions and Future Work

We have presented a method for parallel solution of the fine scale equations in the variational multiscale method based on solution of localized Dirichlet problems on patches and developed an a posteriori error analysis for the method. Based on the estimates we design a basic adaptive algorithm for automatic tuning of the critical parameters: resolution and size of patches in the fine scale problems. It is also possible to decide whether a fine scale computation is necessary or not and thus the proposed scheme may be com-

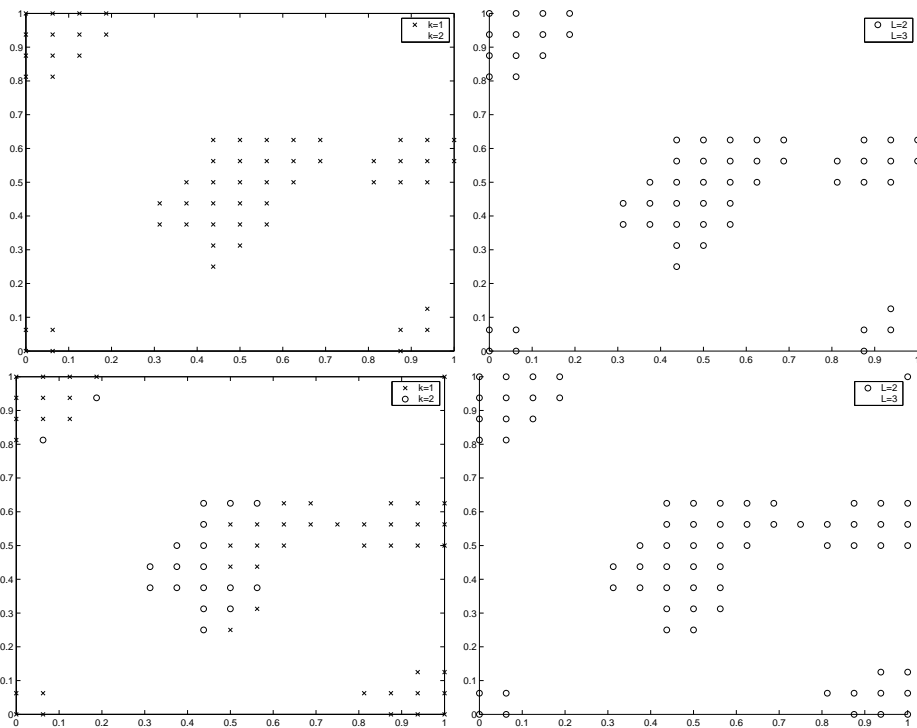


Figure 4: Refinement level,  $h = H \cdot 2^{-k}$ , and number of layers  $L$  for each coarse node. The upper pictures are after one iteration in the adaptive algorithm and the lower pictures are after two iterations.

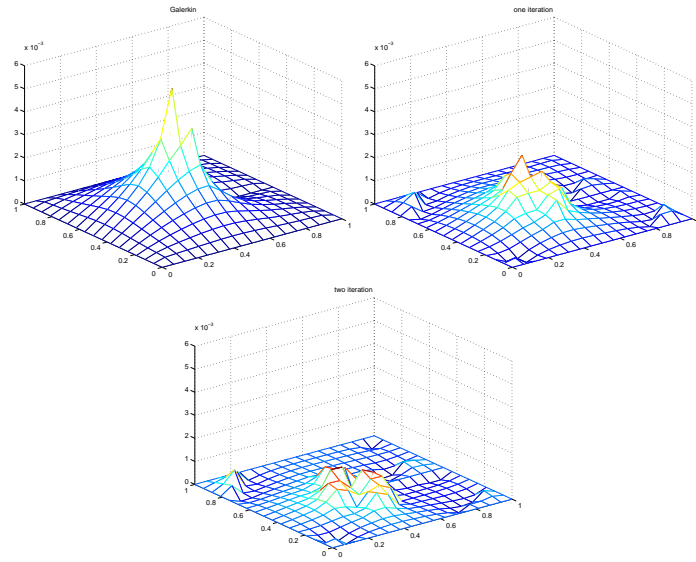


Figure 5: The error in the Galerkin solution (left), after one step in the adaptive algorithm (middle), and after two steps (right).

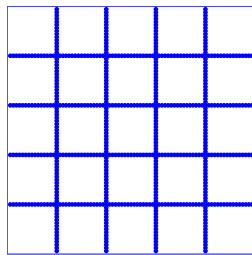


Figure 6: The coefficient is discontinuous with the values  $a = 1$  on the white squares and  $a = 0.05$  on the lattice.

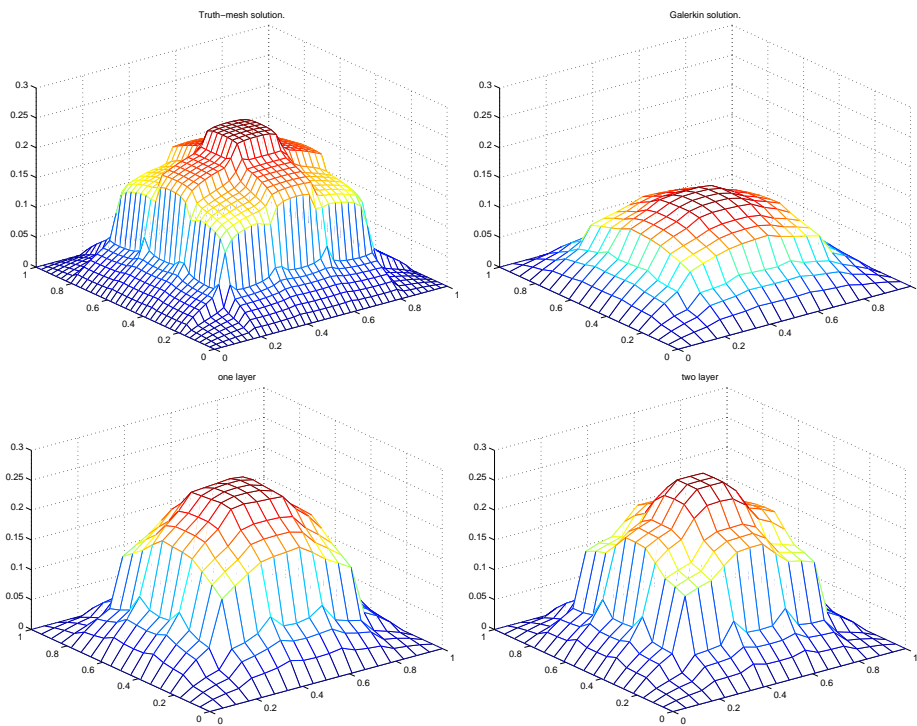


Figure 7: Reference solution (upper left), standard Galerkin on coarse mesh (upper right), solution with local problems using one layer stars (lower left), and finally local problems using two layer stars (lower right).

bined with a standard adaptive algorithm on the coarse scales. The method is thus very general in nature and may be applied to any problem where adaptivity is needed.

In this paper we have focused on two scales in two spatial dimensions. A natural extension would be to solve three dimensional problems with multiple scales. It is also natural to extend this theory to other equations modeling for instance flow and materials.

## References

- [1] T. Arbogast and S. L. Bryant, A two-scale numerical subgrid technique for waterflood simulations, *SPE J.*, Dec. 2002, pp 446-457.
- [2] B. Aksoylu, S. Bond, and M. Holst *An odyssey into local refinement and multilevel preconditioning III: Implementation of numerical experiments*, *SIAM J. Sci. Comput.*, 25(2003), 478-498.
- [3] B. Aksoylu and M. Holst *An odyssey into local refinement and multilevel preconditioning I: Optimality of the BPX preconditioner*, *SIAM J. Numer. Anal.* (2002) in review
- [4] B. Aksoylu and M. Holst *An odyssey into local refinement and multilevel preconditioning II: stabilizing hierarchical basis methods*, *SIAM J. Numer. Anal.* in review
- [5] S. C. Brenner and L. R. Scott, *The mathematical theory of finite element methods*, Springer Verlag, 1994.
- [6] K. Eriksson, D. Estep, P. Hansbo and C. Johnson, *Computational differential equations*, Studentlitteratur, 1996.
- [7] T. Y. Hou and X.-H. Wu, *A multiscale finite element method for elliptic problems in composite materials and porous media*,
- [8] T. J.R. Hughes, *Multiscale phenomena: Green's functions, the Dirichlet-to-Neumann formulation, subgrid scale models, bubbles and the origins of stabilized methods*, *Comput. Methods Appl. Mech. Engrg.* 127 (1995) 387-401.
- [9] T. J.R. Hughes, *The continuous Galerkin method is locally conservative*, *J. Comput. Phys.*, Vol. 163(2) (2000) 467-488.
- [10] T. J.R. Hughes, G. R. Feijóo, L. Mazzei and Jean-Baptiste Quincy, *The variational multiscale method - a paradigm for computational mechanics*, *Comput. Methods Appl. Mech. Engrg.* 166 (1998) 3-24.

- [11] A. A. Oberai and P. M. Pinsky, *A multiscale finite element method for the Helmholtz equation*, Comput. Methods Appl. Mech. Engrg. 154 (1998) 281-297.